

Identification of proteins that are differentially expressed in brains with Alzheimer's disease using iTRAQ labeling and tandem mass spectrometry



Benito Minjarez ^{a,1}, Karla Grisel Calderón-González ^a, Ma. Luz Valero Rustarazo ^{b,2},
María Esther Herrera-Aguirre ^a, María Luisa Labra-Barrios ^a, Diego E. Rincon-Limas ^{c,d},
Manuel M. Sánchez del Pino ^{b,3}, Raul Mena ^{e,4}, Juan Pedro Luna-Arias ^{a,*}

^a Departamento de Biología Celular, Centro de Investigación y de Estudios Avanzados del Instituto Politécnico Nacional (Cinvestav-IPN), Av. Instituto Politécnico Nacional 2508, Col. San Pedro Zacatenco, Gustavo A. Madero, C.P. 07360 Ciudad de México, México

^b Unidad de Proteómica, Centro de Investigación Príncipe Felipe, C/Rambla del Saler 16, 46012 Valencia, España

^c Department of Neurology, McKnight Brain Institute, University of Florida, Gainesville, FL 32611, USA

^d Department of Neuroscience, McKnight Brain Institute, University of Florida, Gainesville, FL 32611, USA

^e Departamento de Fisiología, Biofísica y Neurociencias, Cinvestav-IPN, Av. Instituto Politécnico Nacional 2508, Col. San Pedro Zacatenco, Gustavo A. Madero, C.P. 07360 Ciudad de México, México

ARTICLE INFO

Article history:

Received 5 November 2015

Received in revised form 26 February 2016

Accepted 11 March 2016

Available online 21 March 2016

Keywords:

Alzheimer's disease

Amyloid- β and tau

Drosophila

iTRAQ labeling

Neurofibrillary tangle

Tandem mass spectrometry

ABSTRACT

Alzheimer's disease is one of the leading causes of dementia in the elderly. It is considered the result of complex events involving both genetic and environmental factors. To gain further insights into this complexity, we quantitatively analyzed the proteome of cortex region of brains from patients diagnosed with Alzheimer's disease, using a bottom-up proteomics approach. We identified 721 isobaric-tagged polypeptides. From this universe, 61 were found overexpressed and 69 subexpressed in three brains with Alzheimer's disease in comparison to a normal brain. We determined that the most affected processes involving the overexpressed polypeptides corresponded to ROS and stress responses. For the subexpressed polypeptides, the main processes affected were oxidative phosphorylation, organellar acidification and cytoskeleton. We used *Drosophila* to validate some of the hits, particularly those non-previously described as connected with the disease, such as Sideroflexin and Phosphoglucomutase-1. We manipulated their homolog genes in *Drosophila* models of A β - and Tau-induced pathology. We found proteins that can either modify A β toxicity, Tau toxicity or both, suggesting specific interactions with different pathways. This approach illustrates the potential of *Drosophila* to validate hits after MS studies and suggest that model organisms should be included in the pipeline to identify relevant targets for Alzheimer's disease.

Biological significance: We report a set of differentially expressed proteins in three Alzheimer's disease brains in comparison to a normal brain. Our analyses allowed us to identify that the main affected pathways were ROS and stress responses, oxidative phosphorylation, organellar acidification and cytoskeleton. We validated some identified proteins using genetic models of Amyloid- β and Tau-induced pathology in *Drosophila melanogaster*. With this approach, Sideroflexin and Phosphoglucomutase-1 were identified as novel proteins connected with Alzheimer's disease.

© 2016 Elsevier B.V. All rights reserved.

Abbreviations: AD, Alzheimer's disease; A β , NFT, Neurofibrillary tangle; NPs, Neuritic plaques; PHFs, Paired helical filaments; CSF, Cerebrospinal fluid; PBS, Phosphate buffered saline; GuHCl, Guanidine hydrochloride; ABC, Ammonium bicarbonate; TEAB, Triethylammonium bicarbonate; TCEP, Tris-(2-carboxyethyl) phosphine; MMTS, Methyl methanethiosulfonate; TFA, Trifluoroacetic acid; FA, Formic acid; CHAPS, 3-[(3-Cholamidopropyl)dimethylammonio]-1-propanesulfonate hydrate; ROS, Reactive oxygen species; MS/MS, Tandem mass spectrometry.

* Corresponding author at: Departamento de Biología Celular, Cinvestav-IPN, Av. Instituto Politécnico Nacional 2508, Col. San Pedro Zacatenco, 07360 Ciudad de México, México.

E-mail addresses: bminjarez@hotmail.com (B. Minjarez), karla_grises@hotmail.com (K.G. Calderón-González), mluz.valero@uv.es (M.L.V. Rustarazo), maestherha2@yahoo.com.mx (M.E. Herrera-Aguirre), azu_car2000@yahoo.com.mx (M.L. Labra-Barrios), diego.rincon@neurology.ufl.edu (D.E. Rincon-Limas), sandelpi@uv.es (M.M.S. del Pino), jpluna@cell.cinvestav.mx, jpluna@cinvestav.mx, jpluna2003@gmail.com (J.P. Luna-Arias).

¹ Current Address: Departamento de Biología Celular y Molecular, Centro Universitario de Ciencias Biológicas y Agropecuarias (CUCBA), Universidad de Guadalajara, Camino Ramón Padilla Sánchez No. 2100, Nextipac, Zapopan, Jalisco, México.

² Current Address: Secció de Proteómica, Servei Central de Suport a la Investigació Experimental (SCSIE), Universitat de València, C/Doctor Moliner 50, 46100 Burjassot, València, España.

³ Current Address: Departament de Bioquímica i Biologia Molecular, Facultat de Ciències Biològiques, Universitat de València, C/Doctor Moliner 50, 46100 Burjassot, València, España.

⁴ Deceased.

1. Introduction

There are 36 million people worldwide with dementia and is expected that this number will double by year 2030 [1]. The most common type of dementia in the elderly is Alzheimer's disease (AD), corresponding to approximately 60 to 80% of all cases [2]. AD is a progressive, degenerative and irreversible disorder characterized by cognitive decline and memory loss due to neuronal damage in selected brain regions [3–6]. Pathological hallmarks of AD include the presence of abundant extracellular neuritic plaques (NPs) and intracellular neurofibrillary tangles (NFTs) [4]. NPs are mainly comprised of deposits of aggregated amyloid- β ($A\beta$) [7,8]. NFTs are formed by massive accumulation of abnormal insoluble polymers known as paired helical filaments (PHFs), which are mainly composed of hyperphosphorylated Tau [9–12]. Other pathological features of AD include gliosis, chronic inflammation, excitotoxicity, dysregulation of energy metabolism, oxidative stress, mitochondrial dysfunction, ER stress, and alteration of calcium homeostasis [13–16], which illustrate the complexity of the disease.

Misfolding and accumulation of $A\beta$ in NPs are a critical step in the pathogenesis of AD [4,7,8]. $A\beta$ is formed after sequential proteolytic cleavage of the amyloid- β precursor protein ($A\beta$ PP), which generates several isoforms of 36–43 residues in length [17,18]. The most common isoforms are $A\beta$ 40 and $A\beta$ 42. $A\beta$ 42 is more abundant in NPs and is responsible for the formation of insoluble $A\beta$ fibrillar deposits [18,19]. Nevertheless, soluble $A\beta$ oligomers have shown to be the neurotoxic agents driving AD pathology [20].

Another essential element in AD pathogenesis is Tau. This protein suffers a series of aberrant posttranslational modifications (PTMs) including hyperphosphorylation, ubiquitination, glycosylation, glycation, nitration, and truncation, among others [21]. One of the initial modifications of Tau is abnormal phosphorylation, which leads to a sequence of structural abnormalities resulting in conformational changes, proteolytic cleavage and its accumulation as PHFs [22,23]. Indeed, hyperphosphorylation and aggregation of Tau trigger neuronal microtubule disassembly, leading to axonal transport defects and consequently cell death [24–26]. Albeit Tau is phosphorylated in vitro by numerous protein kinases such as MAPK, GSK-3 β , Cdk5, CaMK, PKA and PKC [21–28], it is unclear how many of these indeed phosphorylate Tau in both physiological and pathological states.

Even though there have been great advances in AD research, the molecular mechanisms, underlying this devastating disease, have not been fully unveiled. Thus, there is a dire need to use novel approaches to better understand the molecular and cellular mechanisms of AD. In addition, different technologies are necessary to decipher the crosstalk between $A\beta$ and Tau and find specific biomarkers that could be useful for measuring risk and progression of AD. One of these technologies is proteomics [29], where Mass Spectrometry (MS) plays a key role in the identification of polypeptides [30]. We recently reported the identification of >100 differentially expressed polypeptides in AD, including GADPH, UCHL-1 and transferrin. GADPH has been previously highlighted as a putative biomarker in AD, while UCHL-1 and transferrin have been related to oxidative stress and iron regulatory processes, respectively [31]. However, this work was essentially qualitative and its main goal was to establish proteomic procedures using both fixed and frozen AD tissues.

Isobaric tags for relative and absolute quantitation (iTRAQ) are being widely used to determine the expression patterns of polypeptides in many biological systems. However, few groups have capitalized on this technique to study AD. For instance, Chen et al. identified twelve subexpressed and seven overexpressed proteins in the substantia

nigra of AD brains in comparison to control samples [32]. Other groups focused on the study of specific proteins and their modifications [33], the polypeptide signature of AD synaptosomes [34] or the search for putative biomarkers in cerebrospinal fluid (CSF) [35]. iTRAQ has been also used in transgenic mouse models of AD. For instance, in the cortex and hippocampus of the 3 \times TgAD mice, there were found 116 and 51 overexpressed polypeptides, while 31 and 42 were subexpressed, respectively [36]. Most of these polypeptides are involved in microtubule dynamics, synaptic plasticity and outgrowth of neurites. Other study identified 24 polypeptides with an expression level significantly altered in 3 \times TgAD mice, some of them corresponding to mitochondrial I and IV complexes from the respiratory chain [37]. Nevertheless, despite all these contributions, there is still an urgent need to quantitatively determine the whole expression profile of polypeptides in the brain of Alzheimer's disease patients in comparison to normal brain.

In this paper we used iTRAQ quantitative proteomics to determine the relative expression levels of polypeptides in AD brains. We identified 721 polypeptides, 61 were overexpressed and 69 subexpressed, which were manually filtered in the human transcriptome database [38] in order to diminish the number of genes, whose expression might be affected by age and sex. This procedure was done because we compared three elder female AD brains with one young male normal brain. Then, we classified them according to their function and validated a selected group of proteins by semiquantitative procedures. Furthermore, their homolog genes were manipulated in *Drosophila* models of $A\beta$ - and Tau-induced pathology to assess their specific involvement in the disease. Surprisingly, we found that some of these proteins can either modify $A\beta$ toxicity, Tau toxicity or both, suggesting specific interactions with different pathological pathways.

2. Methods

2.1. Human brain tissue

In this study we used brains from three Mexican women with Alzheimer's disease of 70, 81 and 87 years old, who showed severe cognition decline and advanced stage of AD. Brains from these individuals were obtained from the Human Brain Bank at Cinvestav-IPN from Mexico, with the approval of the Institutional Humans Subjects Ethics Committee. The postmortem interval for the three cases was 3 h. Diagnosis of AD was performed by the NIA-NINCDS group's criteria [39]. As a control case we used a brain from a 29 years old male, who was a victim of knife injuries. This brain was donated by Dr. Luisa Lilia Rocha Arrieta from Cinvestav-IPN and was previously obtained from the Servicio Médico Forense, Tribunal Superior de Justicia del Distrito Federal (SEMEFO, TSJDF) at Mexico City with a postmortem period of five hours. All brains were frozen immediately after the autopsy at -80°C until use.

2.2. Extraction and quantification of polypeptides

Tissue sections (100 mg) from frozen frontal cortex regions were dissected and used to obtain total homogenates. Samples were resuspended in 300 μL of a solution containing 6 M guanidine hydrochloride (GuHCl) and 0.2 M NH_4HCO_3 pH 7.8 with a portable tissue dispersator using a cordless motor pellet pestle (Sigma-Aldrich), and then homogenized by sonication three times (each 1 min at 60 W of amplitude and keeping on ice for 1 min) using a CPX130PB Ultrasonic Processor (Cole-Parmer). Samples were delipidated three times with a mixture of methanol-chloroform-water (4:1:3; v:v:v), vortexed 1 min at highest

Fig. 1. Identification and quantitation of peptides in brains with Alzheimer's disease by iTRAQ labeling and tandem mass spectrometry. Polypeptides from brains with Alzheimer's disease and from a normal brain were solubilized, trypsin-digested, and iTRAQ-labeled as described. Then, pooled iTRAQ-tagged peptides were separated by isoelectrofocusing in a polyacrylamide gel strip, which was cut in 23 segments. Then, peptides from each segment were extracted and chromatographed through a C-18 RP column and analyzed by tandem mass spectrometry (Materials and Methods). (A) Total ion count of peptides contained in a segment as a function of the elution time as an example. MS/MS spectra for (B) ALTVPELTQQVDFDAK peptide of Tubulin, (C) GYSFTTAAER peptide of Actin, and (D) IGLSDNITHVPGGGNK peptide of Tau. Inserts show the m/z region of tag reporters.

A

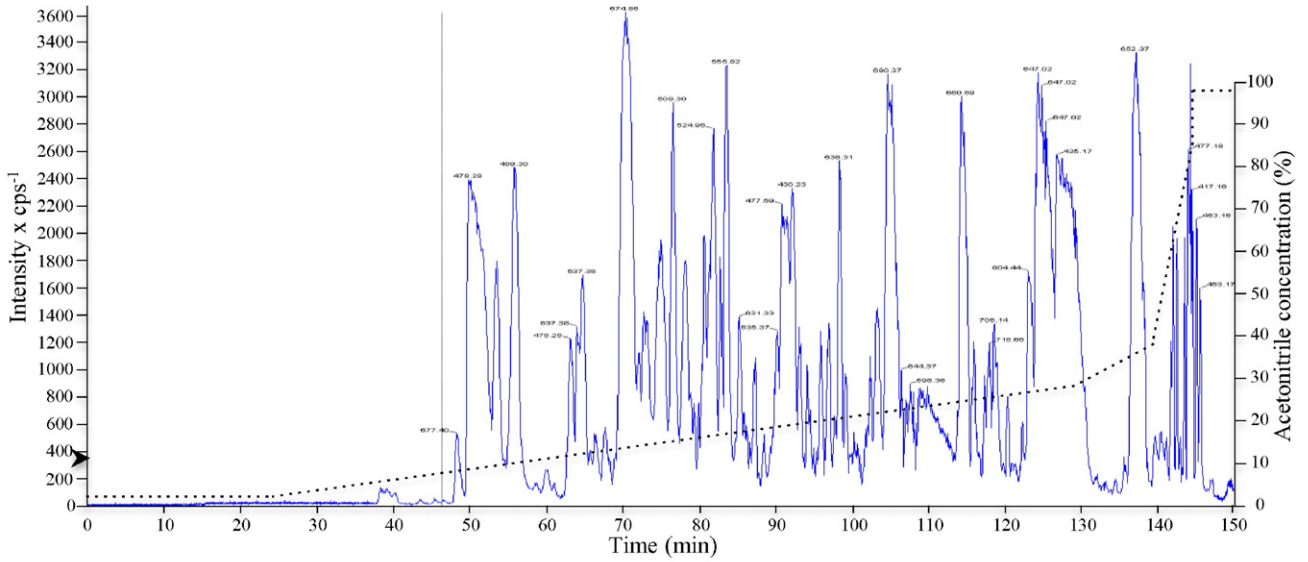


Table 1
Overexpressed polypeptides identified in whole protein extracts of brains with Alzheimer's disease by iTRAQ labeling and tandem mass spectrometry.

Protein name	Gene	UniProtKB ^a acc. no.	MW ^b (kDa)	pI ^c	Pep. Identi. (≥95)	% Cov. ^e (≥95)	114:113 ^f	116:113 ^g	118:113 ^h
1. Glial fibrillary acidic protein	GFAP	P14136	49.88	5.42	68	66.2	1.85	1.49	3.49
2. Collagen alpha-2(I) chain	COL1A2	P08123	129.31	9.08	50	36.2	1.41	1.97	6.10
3. L-Lactate dehydrogenase B chain	LDHB	P07195	36.64	5.71	18	42.5	1.53	1.24	1.21
4. Hemoglobin subunit alpha	HBA1	P69905	15.26	8.72	59	71.8	1.42	2.09	2.92
5. Alpha-1-antitrypsin	SERPINA1	P01009	46.74	5.37	11	29.4	2.84	1.26	1.62
6. Alpha-crystallin B chain	CRYAB	P02511	20.16	6.76	8	58.8	2.37	1.95	1.42
7. Ig gamma-1 chain C region	IGHG1	P01857	36.10	8.46	9	24.2	3.13	1.56	2.25
8. Methylmalonate-semialdehyde dehydrogenase [acylating], mitochondrial	ALDH6A1	Q02252	57.84	8.72	5	9.9	1.29	1.31	1.33
9. Haptoglobin	HP	P00738	45.20	6.13	5	12.3	3.58	1.42	2.29
10. Ferritin light chain	FTL	P02792	20.02	5.50	7	25.7	1.50	1.37	2.65
11. Versican core protein	VCAN	P13611	372.82	4.43	7	2.59	2.35	1.60	2.06
12. Carbonic anhydrase 2	CA2	P00918	29.25	6.87	5	25.0	2.21	1.45	1.23
13. Peroxiredoxin-6	PRDX6	P30041	25.03	6.00	10	29.4	1.45	1.20	1.20
14. Ferritin heavy chain	FTH1	P02794	21.22	5.31	7	22.4	1.88	1.46	1.73
15. Gelsolin	GSN	P06396	85.70	5.90	6	7.6	1.54	1.39	1.89
16. Histone H2B type 1-O	HIST1H2BO	P23527	13.91	10.31	7	27.7	1.25	1.30	1.33
17. Glutathione S-transferase P	GSTP1	P09211	23.36	5.43	4	29.5	2.12	1.50	1.82
18. Histone H3.3	H3F3A	P84243	15.33	11.27	2	11.7	1.30	1.44	1.98
19. Ig alpha-1 chain C region	IGHA1	P01876	37.65	6.08	2	7.0	3.63	2.07	1.63
20. Keratin, type II cytoskeletal 1	KRT1	P04264	66.04	8.15	4	6.0	1.44	1.33	1.33
21. Glutathione S-transferase Mu 1	GSTM1	P09488	25.71	6.24	3	15.1	1.55	1.66	2.25
22. LanC-like protein 1	LANCL1	O43813	45.28	7.86	2	6.2	1.25	1.20	1.36
23. Alpha-1-acid glycoprotein 2	ORM2	P19652	23.60	5.03	2	9.4	4.37	1.75	1.85
24. Protein S100-A1	S100A1	P23297	10.55	4.39	3	38.2	1.20	1.29	1.40
25. Synemin	SYNM	O15061	172.77	5.09	1	0.5	1.45	1.43	2.10
26. 14-3-3 Protein theta	YWHAQ	P27348	27.76	4.68	7	21.2	1.38	1.39	1.33
27. Vacuolar protein sorting-associated protein 33A	VPS33A	Q96AX1	67.61	6.50	1	1.6	2.64	2.71	5.92
28. Vitronectin	VTN	P04004	54.30	5.55	1	3.3	1.31	1.37	3.45
29. Actin, alpha skeletal muscle	ACTA1	P68133	42.05	5.23	37	50.4	1.27	1.38	2.09
30. Ig gamma-2 chain C region	IGHG2	P01859	35.90	7.66	3	10.1	6.39	1.93	2.72
31. T-cell surface glycoprotein CD8 alpha chain	CD8A	P01732	25.73	9.64	1	3.8	1.96	1.45	2.25
32. High mobility group protein B1	HMGB1	P09429	24.89	5.60	1	6.9	1.40	1.38	1.86
33. Nuclease EXOG, mitochondrial	EXOG	Q9Y2C4	41.08	8.45	1	3.2	1.43	1.48	1.25
34. Serum amyloid P-component	APCS	P02743	25.39	6.10	1	5.3	1.89	1.36	5.14
35. Phosphoglucomutase-1	PGM1	P36871	61.45	6.30	1	1.4	1.49	1.21	1.38
36. Complement C4-B	C4B	P0C0L5	192.75	6.89	1	0.5	1.60	1.27	4.50
37. Reticulon-4	RTN4	Q9NQC3	129.93	4.42	2	2.0	3.08	1.52	1.92
38. Argininosuccinate synthase	ASS1	P00966	46.53	8.08	1	1.9	1.35	1.59	5.03
39. Ig kappa chain C region	IGKC	P01834	11.61	5.58	1	16.9	1.95	1.43	1.40
40. Acyl-CoA-binding protein	DBI	P07108	10.04	6.12	1	18.3	1.47	1.45	1.54
41. Melanotransferrin	MF12	P08582	80.21	5.61	1	0.9	5.22	2.29	2.44
42. Peroxiredoxin-1	PRDX1	Q06830	22.11	8.27	11	42.7	1.37	1.15	1.84
43. Superoxide dismutase [Mn], mitochondrial	SOD2	P04179	24.72	8.35	10	43.6	1.21	1.16	1.61
44. Cathepsin D	CTSD	P07339	44.55	6.10	6	16.7	1.26	1.15	1.32
45. Peroxiredoxin-2	PRDX2	P32119	21.89	5.66	9	32.8	1.34	1.15	1.15
46. Annexin A5	ANXA5	P08758	35.94	4.93	4	15.9	1.24	1.16	2.03
47. Heat shock protein beta-1	HSPB1	P04792	27.78	5.98	3	20.0	1.17	1.33	3.07
48. Phosphoserine aminotransferase	PSAT1	Q9Y617	40.42	7.56	2	6.2	1.25	1.15	1.38
49. Alpha-2-macroglobulin	A2M	P01023	163.29	6.03	2	1.9	1.87	1.17	1.96
50. Protein S100-A9	S100A9	P06702	13.24	5.71	3	31.5	1.38	1.15	4.74
51. Prolyl endopeptidase-like	PREPL	Q4J6C6	83.93	5.96	1	1.9	1.18	1.15	1.37
52. Alpha-1-antichymotrypsin	SERPINA3	P01011	47.65	5.33	2	4.9	1.92	1.18	1.34
53. NAD-dependent deacetylase sirtuin-2	SIRT2	Q81XJ6	43.18	5.22	1	4.1	3.12	2.34	1.15
54. Catalase	CAT	P04040	59.76	6.90	1	3.0	1.24	1.17	2.19
55. Galectin-3-binding protein	LGALS3BP	Q08380	65.33	5.12	1	2.9	1.17	1.21	1.77
56. Apolipoprotein A-I	APOA1	P02647	30.78	5.56	1	4.1	1.60	1.16	1.36
57. Ig mu heavy chain disease protein	N/A	P04220	43.06	5.13	1	3.8	1.51	1.17	3.37
58. Heterogeneous nuclear ribonucleoprotein D-like	HNRNPDL	O14979	46.44	9.59	1	1.9	1.15	1.42	1.39
59. WD repeat-containing protein 47	WDR47	O94967	101.95	5.59	1	0.7	1.17	1.05	2.07
60. Alcohol dehydrogenase [NADP+]	AKR1A1	P14550	36.57	6.32	1	3.3	1.34	1.17	1.34
61. Lysine-specific demethylase 4D-like	KDM4E	B2RXH2	56.80	7.95	1	2.5	1.29	1.25	1.17

ADB, Alzheimer's Disease Brain.

N/A, non-assigned.

Bold letters, genes that are differentially expressed as a function of age [52].

^a UniProtKB Acc. Numb., UniProt Knowledgebase accession number.

^b MW, Molecular weight.

^c pI, Isoelectric point.

^d Pep. Ident. (≥95), Number of peptides with at least a confidence of 95% in their identification.

^e % Cov., Percentage of coverage.

^f 114:113, ADB1/Control ratio.

^g 116:113, ADB2/Control ratio.

^h 118:113, ADB3/Control ratio.

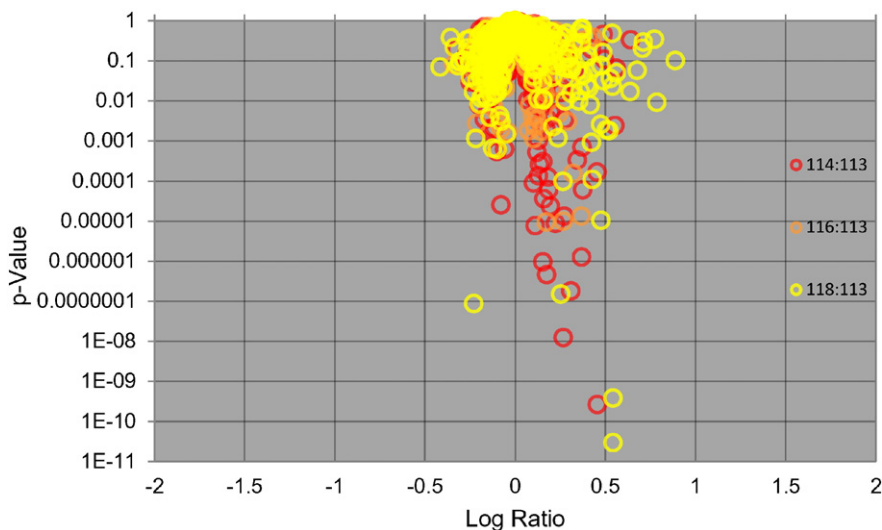


Fig. 2. Volcano plot of proteins identified in Alzheimer's disease brains. Only proteins that were iTRAQ-labeled are shown. X-axis, fold change of polypeptides from brains with Alzheimer's disease, in comparison to a normal brain. Y-axis, statistical significance (*p*-Value) of fold changes. 113 reporter, normal brain; 114 reporter, 70 years old brain (AD1); 116 reporter, 81 years old brain (AD2); 118 reporter, 87 years old brain (AD3).

speed, centrifuged at $12,000 \times g$ for 5 min at room temperature (RT), and methanol precipitated [31]. Pellets were solubilized by sonication in $100 \mu\text{L}$ 8 M urea as mentioned above. Then, proteins were precipitated with 10% trichloroacetic acid (TCA) for 30 min in ice, centrifuged at $12,000 \times g$ for 5 min at 4°C , washed twice with cold acetone (-20°C) and air dried. Polypeptides were solubilized by sonication in $20 \mu\text{L}$ of a solution containing 8 M urea, 0.05% (w/v) ProteaseMAX surfactant Trypsin enhancer (Promega) and 0.5 M triethylammonium bicarbonate (TEAB) pH 8.0 as described. Finally, protein concentration was determined by the Bradford method [40] and samples stored at -20°C until use.

2.3. Trypsin digestion of polypeptides and iTRAQ labeling

Before the labeling with isobaric tags, $110 \mu\text{g}$ of each sample were mixed with 0.5 M TEAB up to a final volume of $40 \mu\text{L}$, reduced with 50 mM Tris-(2-carboxyethyl) phosphine hydrochloride (TCEP) reducing agent at 37°C for 1 h, and alkylated with 200 mM *S*-methyl methanethiosulfonate (MMTS) for 10 min at RT, following the protocol described in the iTRAQ Reagents – 8plex labeling manual (AB SCIEX) with minor modifications. Then, urea concentration in samples was reduced to <2 M with 0.5 M TEAB, digested with $10 \mu\text{g}$ of sequencing grade modified trypsin (Promega) overnight at 37°C , and dried in a Savant SpeedVac concentrator (Thermo Scientific) at 60°C for 1 h. Each sample was labeled with an isobaric tag for 3 h at RT as follows: case control with the 113 tag, the 70 years old brain (AD1) with 114 tag, 81 years old brain (AD2) was tagged 116, and the 87 years old brain (AD3) with the 118 tag. Finally, all samples were pooled before application of separation techniques and analysis by tandem mass spectrometry.

2.4. Separation of peptides by isoelectrofocusing in a polyacrylamide gel and C18 reverse phase column chromatography

To diminish the complexity of samples, we performed an isoelectrofocusing (IEF) separation procedure in 13 cm polyacrylamide gel strips containing a mixture of ampholytes forming a nonlinear pH 3–10 gradient (GE Healthcare) under denaturing conditions, using an Ettan IPGphor 3 IEF System (GE Healthcare). Isoelectrofocusing conditions used were $75 \mu\text{A}$ per strip at 20°C , using 5000 V, 30,000 V h, followed by 500 V for 30 h. Then, strips were washed with deionized water, cut into 23 small strips, each 0.5 cm wide, and peptides from each piece

were sequentially extracted with $50 \mu\text{L}$ of a) 0.1% trifluoroacetic acid (TFA), b) a solution of 50% acetonitrile (ACN) and 0.1% TFA, and c) 0.1% TFA in ACN, each for 10 min at RT. All peptide solutions obtained for each small strip were pooled and vacuum-dried, solubilized in 0.1% TFA, cleaned with Poros R2 tips (home-made) and eluted with $40 \mu\text{L}$ of 75% ACN and 0.1% TFA solution. Finally, samples were vacuum-concentrated to $3 \mu\text{L}$ and diluted with $12 \mu\text{L}$ of 5% ACN and 0.1% TFA solution.

2.5. Tandem mass spectrometry analysis

The mass spectrometer was calibrated with 200 fmol of a mixture of six polypeptides digested with trypsin (*E. coli* β -galactosidase; *Bos taurus* serotransferrin, serum albumin, and cytochrome C; *Saccharomyces cerevisiae* alcohol dehydrogenase 1; *Gallus gallus* lysozyme C. All of them were purchased from LC Packings, Amsterdam, NL). Conditions that were used in this calibration were also used for the analysis of problem samples (described below). Identification of calibration peptides was performed with the Mascot Daemon software (Matrix Science, London, UK). Tagged peptides were concentrated onto a PepMap C18 trap cartridge ($300 \mu\text{m} \times 5 \text{ mm}$, LC Packings) using as mobile phase 0.1% TFA for 10 min and an isocratic flow rate of $30 \mu\text{L}/\text{min}$. Then, peptides were separated through a silica nanoBaume C18 reverse phase (RP) analytical chromatography column ($75 \mu\text{m} \times 50 \text{ cm}$, $5 \mu\text{m}$ particle size, home-made), using the next ACN lineal gradients in 0.1% formic acid (FA): 1) 1.9% to 28.5% in 105 min, 2) 28.5% to 38% in 10 min, and 3) 38% to 85.5% in 5 min. Finally, a final elution step was performed using an isocratic flow of 98% ACN for 5 min. All reverse phase steps were run at a flow rate of 250 nL/min. As peptides were eluted from the analytical RP column, they were immediately injected and analyzed in a high performance hybrid quadrupole time-of-flight mass spectrometer (QSTAR ESI XL Hybrid LC/MS/MS Mass Spectrometer System, AB SCIEX, Madrid, Spain) from the Centro de Investigación Príncipe Felipe, Valencia, Spain, using the Analyst QS 1.1 software (AB SCIEX, Madrid, Spain). Information Dependent Acquisition (IDA) experiments were performed in all chromatograms. Collected mass spectra were used to identify (with the Paragon algorithm) and quantify (using the ProGroup algorithm) peptides as well as the False Discovery Rate (FDR) with the ProteinPilot software version 4.0 (AB SCIEX, Mexico City, Mexico) using the UniProtKB/Swiss-Prot Human database (UniProt Knowledgebase, Human Sprot_20120120.fasta, www.uniprot.org). Analysis parameters were peptide label (iTRAQ 8plex), trypsin

Table 2
Subexpressed polypeptides identified in whole protein extracts of brains with Alzheimer's disease by iTRAQ labeling and tandem mass spectrometry.

Protein name	Gene	UniProtKB ^a acc. no.	MW ^b (kDa)	pI ^c	Pep. ^d ident. (≥95)	% Cov. ^e (≥95)	114:113 ^f	116:113 ^g	118:113 ^h
1. Annexin A6	ANXA6	P08133	75.87	5.41	5	9.8	0.76	0.79	0.76
2. T-complex protein 1 subunit beta	CCT2	P78371	57.49	6.01	4	11.2	0.73	0.70	0.56
3. Synapsin-2	SYN2	Q92777	62.85	8.58	6	10.8	0.73	0.61	0.60
4. Neuronal cell adhesion molecule	NRCAM	Q92823	143.89	5.45	4	3.9	0.83	0.85	0.70
5. NADH dehydrogenase [ubiquinone] iron-sulfur protein 3, mitochondrial	NDUFS3	O75489	30.24	6.98	5	16.6	0.71	0.82	0.76
6. Disks large homolog 4	DLG4	P78352	80.50	5.58	2	2.6	0.67	0.67	0.64
7. 2-oxoglutarate dehydrogenase-like, mitochondrial	OGDHL	Q9ULD0	114.48	6.18	2	2.8	0.72	0.82	0.70
8. ADP/ATP translocase 3	SLC25A6	P12236	32.87	9.76	5	19.1	0.57	0.69	0.59
9. DnaJ homolog subfamily C member 11	DNAJC11	Q9NVH1	63.28	8.54	2	5.9	0.79	0.67	0.67
10. NADH dehydrogenase [ubiquinone] iron-sulfur protein 8, mitochondrial	NDUFS8	O00217	23.70	6.00	2	9.5	0.63	0.82	0.38
11. ATP synthase subunit f, mitochondrial	ATP5J2	P56134	10.92	9.70	2	25.5	0.62	0.74	0.81
12. V-type proton ATPase subunit D	ATP6V1D	Q9Y5K8	28.26	9.36	2	13.7	0.77	0.82	0.69
13. Glutaminase kidney isoform, mitochondrial	GLS	O94925	73.46	7.85	2	4.6	0.63	0.85	0.64
14. V-type proton ATPase 116 kDa subunit a isoform 1	ATP6V0A1	Q93050	96.41	6.01	2	3.3	0.70	0.81	0.85
15. Kinesin heavy chain isoform 5C	KIF5C	Q60282	109.49	5.86	2	2.2	0.76	0.68	0.62
16. Copine-5	CPNE5	Q9HCH3	65.73	5.65	2	4.7	0.72	0.80	0.79
17. UMP-CMP kinase	CMPK1	P30085	22.22	5.44	4	20.9	0.61	0.61	0.46
18. Tubulin alpha-1A	TUBA1A	Q71U36	50.14	4.94	84	50.5	0.74	0.58	0.48
19. AP-2 complex subunit mu	AP2M1	Q96CW1	49.65	9.57	2	6.2	0.71	0.78	0.66
20. V-type proton ATPase subunit F	ATP6V1F	Q16864	13.37	5.29	4	34.4	0.83	0.78	0.51
21. Astrocytic phosphoprotein PEA-15	PEA15	Q15121	15.04	4.93	2	26.9	0.79	0.62	0.57
22. Cytochrome c oxidase subunit 2	MT-CO2	P00403	25.56	4.67	1	8.8	0.56	0.71	0.72
23. Ubiquitin carboxyl-terminal hydrolase 5	USP5	P45974	95.79	4.91	3	5.7	0.67	0.81	0.80
24. Dihydropyridyllysine-residue succinyltransferase component of 2-oxoglutarate dehydrogenase complex, mitochondrial	DLST	P36957	48.76	9.10	2	5.5	0.80	0.79	0.68
25. Hydroxyacylglutathione hydrolase, mitochondrial	HAGH	Q16775	33.80	8.34	2	7.7	0.70	0.56	0.54
26. Neural precursor cell expressed developmentally down-regulated protein 8	NEDD8	Q15843	9.07	7.99	3	25.9	0.82	0.82	0.49
27. Dynamin-like 120 kDa protein, mitochondrial	OPA1	O60313	111.63	7.87	3	2.6	0.79	0.78	0.84
28. NADH dehydrogenase [ubiquinone] 1 alpha subcomplex subunit 13	NDUFA13	Q9P0J0	16.70	8.02	1	9.0	0.53	0.61	0.49
29. Beta-soluble NSF attachment protein	NAPB	Q9H115	33.56	5.32	1	3.6	0.75	0.72	0.43
30. A-kinase anchor protein 12	AKAP12	Q02952	191.48	4.37	1	0.8	0.66	0.69	0.65
31. N-terminal EF-hand calcium-binding protein 2	NECAB2	Q726G3	43.19	5.32	1	2.8	0.54	0.45	0.62
32. Transforming protein RhoA	RHOA	P61586	21.77	5.83	3	8.8	0.70	0.69	0.73
33. Sideroflexin-1	SFXN1	Q9H9B4	35.62	9.22	1	2.7	0.47	0.73	0.52
34. AP-2 complex subunit alpha-2	AP2A2	O94973	103.96	6.53	4	5.4	0.71	0.68	0.67
35. Solute carrier family 12 member 5	SLC12A5	Q9H2X9	126.18	6.29	1	1.9	0.70	0.71	0.59
36. Guanine nucleotide-binding protein G(k) subunit alpha	GNAI3	P08754	40.53	5.50	5	15.2	0.62	0.79	0.59
37. Ras-related protein Rab-3C	RAB3C	Q96E17	25.95	5.09	3	16.3	0.58	0.62	0.59
38. Ubiquilin-2	UBQLN2	Q9UHD9	65.70	5.15	1	2.4	0.67	0.76	0.76
39. Excitatory amino acid transporter 2	SLC1A2	P43004	62.10	6.09	1	2.6	0.53	0.73	0.78
40. Protein KIAA1045	KIAA1045	Q9UPV7	45.19	5.48	1	2.5	0.51	0.70	0.64
41. Small glutamine-rich tetratricopeptide repeat-containing protein alpha	SGTA	O43765	34.06	4.79	2	4.4	0.74	0.76	0.75
42. Single-stranded DNA-binding protein, mitochondrial	SSBP1	Q04837	17.26	9.59	1	10.1	0.69	0.65	0.64
43. NADH dehydrogenase [ubiquinone] flavoprotein 2, mitochondrial	NDUFV2	P19404	27.39	8.22	1	5.2	0.63	0.78	0.57
44. Drebrin	DBN1	Q16643	71.43	4.40	1	4.3	0.62	0.53	0.54
45. Phosphatidylinositol-5-phosphate 4-kinase type-2 gamma	PIP4K2C	Q8TBX8	47.30	6.36	1	3.5	0.75	0.79	0.69
46. 26S protease regulatory subunit 10B	PSMC6	P62333	44.17	7.09	1	3.5	0.59	0.80	0.77
47. Heterogeneous nuclear ribonucleoprotein H3	HNRNPH3	P31942	36.93	6.37	1	2.8	0.52	0.61	0.63
48. EF-hand domain-containing protein D2	EFHD2	Q96C19	26.70	5.15	1	2.9	0.75	0.65	0.66
49. Dihydropyrimidinase-related protein 5	DPYSL5	Q9BPU6	61.42	6.73	2	2.4	0.70	0.69	0.71
50. Serine/threonine-protein kinase DCLK1	DCLK1	O15075	82.22	8.84	1	1.3	0.63	0.67	0.79
51. Sodium-driven chloride bicarbonate exchanger	SLC4A10	Q6U841	125.95	6.05	1	0.9	0.27	0.70	0.42
52. Ras-related protein Rab-15	RAB15	P59190	24.39	5.53	2	9.9	0.74	0.67	0.66
53. Electrogenic sodium bicarbonate cotransporter 1	SLC4A4	Q9Y6R1	121.46	6.35	1	2.2	0.53	0.69	0.67
54. Bis(5'-nucleosyl)-tetrphosphatase [asymmetrical]	NUDT2	P50583	16.83	5.23	1	5.4	0.73	0.68	0.67
55. Copine-2	CPNE2	Q96FN4	61.19	5.71	1	1.6	0.63	0.57	0.60
56. Dynamin-1	DNM1	Q05193	97.41	6.73	20	20.0	0.79	0.81	0.77
57. ADP/ATP translocase 1	SLC25A4	P12235	33.06	9.78	7	22.1	0.60	0.81	0.78
58. Histone H2A type 2-A	HIST2H2AA3	Q6F113	14.10	10.90	9	49.2	0.81	0.70	0.70
59. Dihydropyrimidinase-related protein 1	CRMP1	Q14194	62.18	6.55	13	19.5	0.83	0.75	0.63
60. Tubulin beta-2 A chain	TUBB2A	Q13885	49.91	4.78	92	62.2	0.81	0.76	0.56
61. Prohibitin	PHB	P35232	29.80	5.57	6	27.2	0.78	0.84	0.61
62. Microtubule-associated protein 2	MAP2	P11137	199.53	4.82	4	3.1	0.77	0.85	0.68
63. 116 kDa U5 small nuclear ribonucleoprotein component	EFTUD2	Q15029	109.44	4.84	1	1.3	0.83	0.78	0.72
64. 6-phosphogluconate dehydrogenase, decarboxylating	PGD	P52209	53.14	6.80	1	4.7	0.85	0.84	0.84
65. Cyclin-G-associated kinase	GAK	O14976	143.19	5.49	1	1.2	0.67	0.82	0.56
66. 40S ribosomal protein S15a	RPS15A	P62244	14.84	10.14	1	6.9	0.51	0.72	0.85
67. Carnitine O-palmitoyltransferase 1, liver isoform	CPT1A	P50416	88.37	8.85	1	1.5	0.32	0.70	0.83
68. Calcium/calmodulin-dependent protein kinase type II subunit beta	CAMK2B	Q13554	72.68	6.87	5	10.0	0.69	0.81	0.41
69. Zinc finger protein 606	ZNF606	Q8WXB4	91.81	8.16	1	0.75	0.80	0.70	0.83

specificity allowing one missed cleavage, cysteine alkylation (MMTS), special factors (urea denaturation), search effort (thorough) and FDR analysis. Carbamidomethylation of Cys (C(CAM)) was used as a fixed modification, and oxidation of methionine and deamidation of asparagine and glutamine as variable modifications. A tolerance on the mass measurement of 100 ppm in MS mode and ± 0.5 Da for MS/MS ions were used in our analysis. Reliability percentage of identified proteins was $\geq 95\%$ (score of 1.30). For quantification, we used the denominator iT113 and the automatic bias correction. To determine significant changes in the protein expression level we performed the analysis with the ProteinPilot Descriptive Statistics Template (PDST) v. 3.001p (AB SCIEX, Mexico City, Mexico). Data were also exported to an Excel worksheet for manual analysis. Proteins with > 1.15 -fold change were considered overexpressed, and < 0.85 -fold change were subexpressed. Finally, selected proteins were manually filtered using data of the human transcriptome database [38] to diminish the number of genes whose expression might be affected by age and sex. This had to be performed because we used three AD brains from old women and one young male normal brain as a control.

2.6. Bioinformatics analysis

The polypeptides that changed in their expression level were grouped in Venn-Euler diagrams using the Venny program (<http://bioinfogp.cnb.csic.es/tools/venny/>). To classify these proteins we used the PANTHER (Protein Annotation Through Evolutionary Relationship) classification system v 10.0 (<http://www.pantherdb.org/>), according to their role in biological processes [41]. The identification of the functional interaction networks was performed with the STRING (Search Tool for the Retrieval of Interacting Genes/Proteins) program (version 10.0; <http://string-db.org/>). Active prediction methods were neighborhood, coexpression, gene fusions, experiments, cooccurrence, databases and text mining, using high confidence (0.7).

2.7. IPA core analysis

In order to classify the identified proteins involved in diseases and biological functions, canonical pathways, molecular networks and the selection of putative candidates for biomarkers, we used the module Core Analyses and Biomarkers filter of the full version of the Ingenuity Pathway Analysis software (IPA, QIAGEN's Redwood City, www.qiagen.com/ingenuity). We performed only one analysis named Core II. Core II analysis included cells as astrocytes and neurons, nervous system, as well as Central Nervous System (CNS) and neuroblastoma cell lines using the stringent filter, and included the next parameters: 1) Ingenuity Knowledge Base (genes only), considering direct and indirect relationships. 2) Interaction networks including endogenous chemicals, default value of 35 molecules per network and 25 networks per analysis. 3) All data sources. 4) Confidence: experimentally observed, highly and moderately predicted. 5) Human species with stringent filter. 6) All mutations. The Fisher's Exact Test was used to determine the *p*-Value, which was considered as significant with values lower than 0.05.

2.8. IPA biomarker analysis

For selection of some putative biomarkers, we filtered all selected proteins through IPA software using the Biomarkers II and III analyses. In Biomarkers II we focused on the analyses in tissues and primary cells, including astrocytes and neurons, nervous system, as well as CNS and neuroblastoma cell lines. The diseases considered in this filter were neurological diseases and psychological disorders. All biomarker applications were considered as well as neurological diseases and psychological disorders. Biomarkers III parameters were the same of Biomarkers II, except for all biomarkers application that only included Alzheimer in neurological diseases. All filters included the next parameters: 1) Human species, 2) all molecules type, and 3) all biofluids. On the other hand, we compared the putative biomarkers obtained in all filters using the Venny program.

2.9. Western blot analysis

Total homogenate samples (100 μ g per lane) were electrophoresed in 12% SDS-PAGE gels in a MiniProtean Tetra Cell (Bio-Rad) at 100 V. Then, polypeptides were transferred to nitrocellulose membranes (GE Amersham) in a Mini Trans-Blot Electrophoretic Transfer Cell (Bio-Rad) using Tris-glycine buffer (25 mM Tris, 192 mM glycine, pH 8.3) containing 20% methanol (v/v) at 40 V overnight at 4 °C. Transference of polypeptides was verified by staining with Ponceau Red and destained by extensively rising with plenty of $1 \times$ PBS containing 0.05% (v/v) Tween 20 (PBS-T). Next, membranes were blocked with 5% Skim Milk (Difco) in PBS-T overnight at 4 °C with gentle agitation and incubated with primary antibodies in 3% (w/v) Bovine Serum Albumin (BSA) in PBS-T overnight at 4 °C. Primary antibodies used were mouse *anti-Tau* 7.51 (a gift from Dr. Claude M. Wischik and Dr. Charles R. Harrington from the University of Aberdeen, UK) diluted 1:20, mouse *anti-tubulin* (1:1000, Invitrogen), mouse *anti-ferritin heavy chain* (1:300, Santa Cruz Biotechnology), mouse *anti-actin* (1:1000, a gift from Dr. José Manuel Hernandez from Cinvestav-IPN, Mexico), mouse *anti-HSP60* (5 μ g/mL, Millipore), mouse *anti-HSP70* (1 μ g/mL, Millipore), and mouse *anti-HSP90* (0.5 μ g/mL, Millipore). Membranes were washed 10 times with PBS-T for 10 min each at RT, and incubated with horseradish peroxidase (HRP)-coupled secondary antibodies (goat anti-mouse, 1:20,000, Vector Labs.) in 2% BSA (w/v) in PBS-T containing StrepTactin-HRP Conjugate (1:10,000, Bio-Rad) for 1 h at RT with gentle agitation. Finally, membranes were revealed with the ECL Plus kit (Amersham) and High Performance Chemiluminescence Films (GE Healthcare). Digital images of Western blots were obtained with the Gel Doc EZ Imager system and processed with the Image Lab software version 3.0 (both from Bio-Rad). As molecular mass markers we used the Strep-tagged Precision Plus Protein All Blue Standards (Bio-Rad).

2.10. Drosophila stocks and genetics

The eye-specific driver *gmr-Gal4*, UAS-lacZ reporter (control), the UAS-based dsRNA lines for silencing PGM1 (BDSC#34345) and Rho1 (BDSC#9909), as well as the *P*-element strain carrying an insertion in

Notes to Table 2

Bold names, genes that are differentially expressed as a function of age [52].

^a UniProtKB Acc. No., UniProt Knowledgebase accession number.

^b MW, Molecular weight.

^c pI, Isoelectric point.

^d Pep. Ident. (≥ 95), number of peptides with at least 95% of confidence in their identification.

^e % Cov., percentage of coverage.

^f 114:113, ADB1/control ratio.

^g 116:113, ADB2/control ratio.

^h 118:113, ADB3/control ratio.

the Sideroflexin orthologue (CG11739^{d06383}, BDSC#19236) were obtained from the Bloomington Drosophila Stock Center in Indiana, U.S.A. The UAS line expressing A β 42 fused to a signal peptide for secretion was previously outlined [42]. The UAS-Tau flies express the longest human Tau isoform (4N2R) and were kindly provided by Matt Mahoney from Vitruvean, Inc. After generating recombinant stocks carrying *gmr-Gal4*, UAS-A β 42/Cyo and *gmr-Gal4*, UAS-Tau/Cyo, virgins were collected and crossed with males from the aforesaid control and candidate stocks at 26 °C.

2.11. Drosophila eye imaging

Eye phenotypes resulting from the crosses described above were imaged using 1 day-old males. To do so, flies eclosed during a 24 h period were frozen at -80°C overnight. Then, eye images were collected as Z-stacks with a Leica Z16 APO using a $2\times$ Plan-Apo objective and single in-focus images were generated with the Montage Multifocus module of the Leica Application Software.

3. Results

3.1. Quantitative proteomic analysis of brains with Alzheimer's disease

In a previous report, we identified 102 polypeptides and 41 proteins from total homogenates and NFTs isolated by laser capture microdissection, respectively, from a brain with Alzheimer's disease, using C-18 reverse phase chromatography as an initial separation step of peptides, and tandem mass spectrometry [31]. The aim of this new study is to identify and quantify the polypeptides that showed a change in their relative expression levels within AD and normal brains. To that end, we used isobaric tag labeling and two methods to diminish sample complexity, isoelectrofocusing and reverse phase chromatography, followed by tandem mass spectrometry. The elution patterns of ions were obtained from 38 to 150 min (Fig. 1A). The assignment and quantification of the peptides was based on the collected MS/MS spectra. The spectra of peptides ALVPELTQQVFDK, GYSFTTAAER, and IGLSDNITHVPGGGNK, which belong to Tubulin, Actin, and Tau, respectively, are shown as examples (Fig. 1B–D). We identified 721 polypeptides, which were recognized using at least one peptide with equal or $>95\%$ in confidence (Table 1 in Ref [43]). The list of proteins was exported to a PDST template to determine the FDR and plot them according to their log ratio and p -values as a volcano plot (Fig. 2). We set the cut-off values of ≥ 1.15 and ≤ 0.85 to classify the identified polypeptides as overexpressed and subexpressed proteins in the three AD brains in comparison to a normal brain, respectively, and select them for further analyses. We obtained 61 overexpressed proteins (Table 1) and 69 subexpressed polypeptides (Table 2). These proteins were manually curated by filtering in the human transcriptome database [38] to discard those polypeptides whose expression is dependent on age and sex (see Tables 1 and 2, bold gene names). It is necessary to emphasize that even after to have filtered the data, these might exclude potential positive data and also could include false positive data. This procedure had to be done to reduce false positive proteins related to sex and age because we compared three female AD brains aged between 70 and 87 years old with a normal brain from a 29 years old male. Hence 10 proteins (A2M, CA2, CD8A, HBA1, HSPB1, LDHB, PGM1, RTN4, VPS33A, and YWHAQ) were found in the overexpressed set, and 7 polypeptides in the subexpressed group (CCT2, NDUFS3, NDUFV2, OPA1, SLC25A4, SSBP1, and TUBA1A), whose expression level is age-dependent (Table S12 in [38]). There were not identified genes whose expression is sex-related (Table S10 in [38]).

3.2. Functional classification of overexpressed and subexpressed polypeptides from AD brains

The proteins that changed in their expression levels were classified with the PANTHER Classification System. Overexpressed proteins were

grouped into 24 protein classes containing 81 protein class hits. The category with more hits was Oxidoreductase (XIV), which had 9 polypeptides (Fig. 3A). In the case of the classification into biological processes, we obtained 12 categories with 135 hits. The Metabolic Process (IX) was the category most represented with 32 polypeptides (Fig. 3B). In relation to the subexpressed polypeptides, we got 19 categories that grouped 79 protein hits, being the Hydrolase class (VIII) the category with more proteins (Fig. 3C). For biological processes we got 12 categories with a total of 136 process hits. The Metabolic Process class (X) was the category with the biggest number of proteins (44) (Fig. 3D).

3.3. Putative interaction networks determined by String analysis

To determine the putative interaction networks of the differentially expressed polypeptides, we performed an analysis with the String software. The overexpressed protein network involved 15 biological processes, all with a p value ≤ 0.05 , being the main processes: 1) Response to stress, 2) catabolic process, 3) response to inorganic substance and single catabolic processes, 4) response to oxidative stress, and 5) response to wounding (Fig. 4). In relation to the subexpressed polypeptides, we got a network that involved 20 processes with statistical significance ($p \leq 0.05$). The main processes involved were: 1) Nucleobase-containing small molecule metabolic process, 2) energy derivation by oxidation of organic compounds, 3) generation of precursor metabolites and energy, and nucleoside phosphate metabolic processes, 4) cellular respiration, ribonucleotide and nucleotide metabolic processes, and glycosyl compound metabolic processes, among others (Fig. 5).

3.4. IPA analysis

In order to classify the overexpressed or subexpressed polypeptides according to diseases and biofunctions, as well as functional networks, we performed an analysis with the IPA software only for Core II, which was executed only in cells, including astrocytes and neurons, nervous system, as well as CNS, and neuroblastoma cell lines. For the classification according to diseases and biofunctions, Core II analysis revealed 26 categories with a significant p -Value ($p < 0.05$, Table 3). Thus, identified proteins are involved in: a) Neurological Disease (32 molecules with p -Values of 4.53×10^{-7} to 4.48×10^{-2}), b) Psychological Disorders (30 proteins with p -Values between 1.81×10^{-6} and 4.48×10^{-2}), c) Metabolic Diseases (11 polypeptides and p -Values from 2.54×10^{-6} to 9.12×10^{-3}), and d) Skeletal and Muscular Disorders (13 proteins with p -Values of 2.58×10^{-6} to 8.49×10^{-3}).

For the functional classification, the most representative functional networks generated with the Core II analysis were related to: 1) Cell Death And Survival, Free Radical Scavenging, Cellular Growth And Proliferation, Cell Morphology, Cellular Function And Maintenance, Cellular Movement, Dna Replication, Recombination, And Repair. This network was focused on 12 proteins and had a score of 12 (Fig. 6A). 2) The second network was related to Free Radical Scavenging, Cardiovascular Disease, Cell Death and Survival, Cancer, and Cell Morphology with 6 polypeptides and a score of 7 (Fig. 6B).

To prioritize putative biomarkers for AD, we first filtered proteins, eliminating those related proteins that undergo a change in their expression level as a function of age. Then, we performed a filtration of the proteins with the IPA software. Biomarker II filter was performed in astrocytes and neurons, nervous system, as well as CNS and neuroblastoma cell lines, all biomarkers applications and biomarkers diseases, including neurological diseases and psychological disorders. In this case, there were 10 polypeptides selected: ALDH6A1, APOA1, CRYAB, CTSD, DLG4, GFAP, HNRNPDL, PRDX6, RAB11A, and SERPINA1. Finally, the analysis of Biomarkers III included astrocytes and neurons, nervous system, as well as CNS and neuroblastoma cell lines, besides all biomarkers applications and biomarkers diseases, which considered neurological

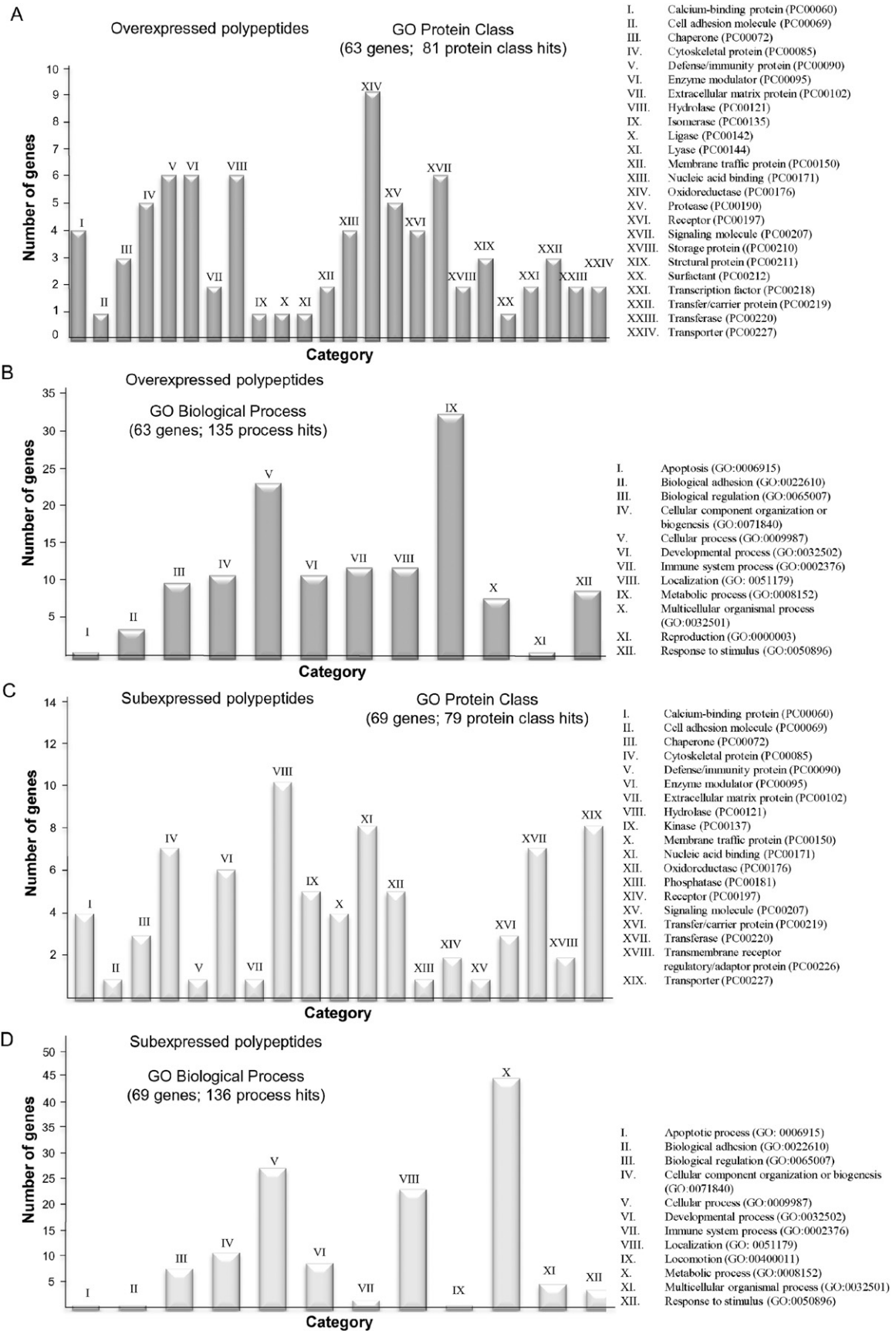
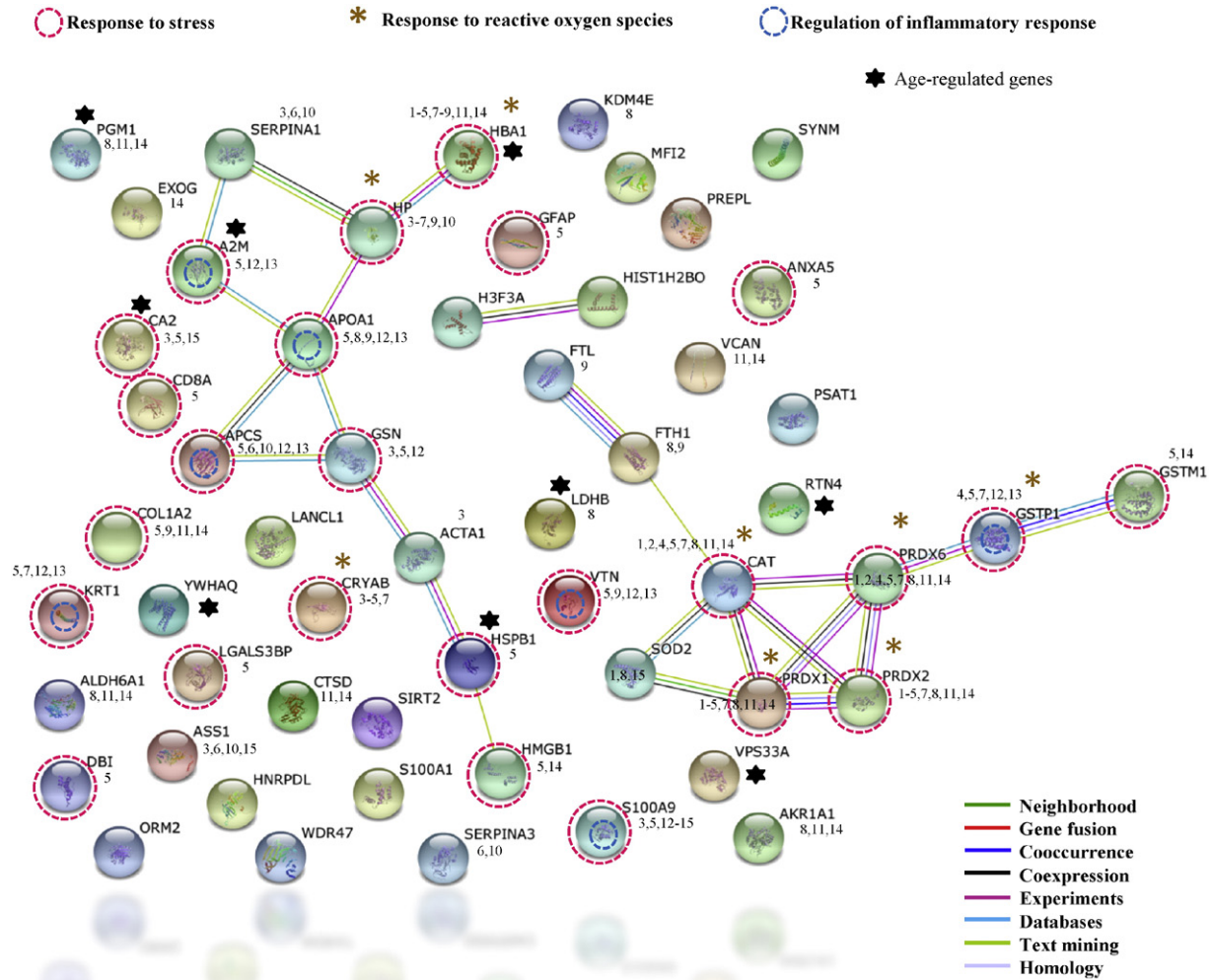


Fig. 3. PANTHER-based functional classification of differentially expressed polypeptides found consistently in brains with Alzheimer's disease. The UniProtKB IDs of overexpressed (A, B) and subexpressed (C, D) proteins were submitted to the PANTHER database for their classification in Gene Ontology (GO) according to Protein Class (A, C) and Biological Process (B, D). X-axis, categories of proteins. Y-axis, number of genes contained in each category.



- | | |
|--|--|
| <ol style="list-style-type: none"> 1. Hydrogen peroxide metabolic process (6) 2. Hydrogen peroxide catabolic process (5) 3. Response to inorganic substance (11) 4. Response to reactive oxygen species (8) 5. Response to stress (25) 6. Acute-phase response (5) 7. Response to oxidative stress (9) 8. Oxidation-reduction process (13) | <ol style="list-style-type: none"> 9. Receptor-mediated endocytosis (7) 10. Acute inflammatory response (5) 11. Single-organism catabolic process (11) 12. Regulation of response to wounding (8) 13. Regulation of inflammatory response (7) 14. Catabolic process (15) 15. Response to zinc ion (4) |
|--|--|

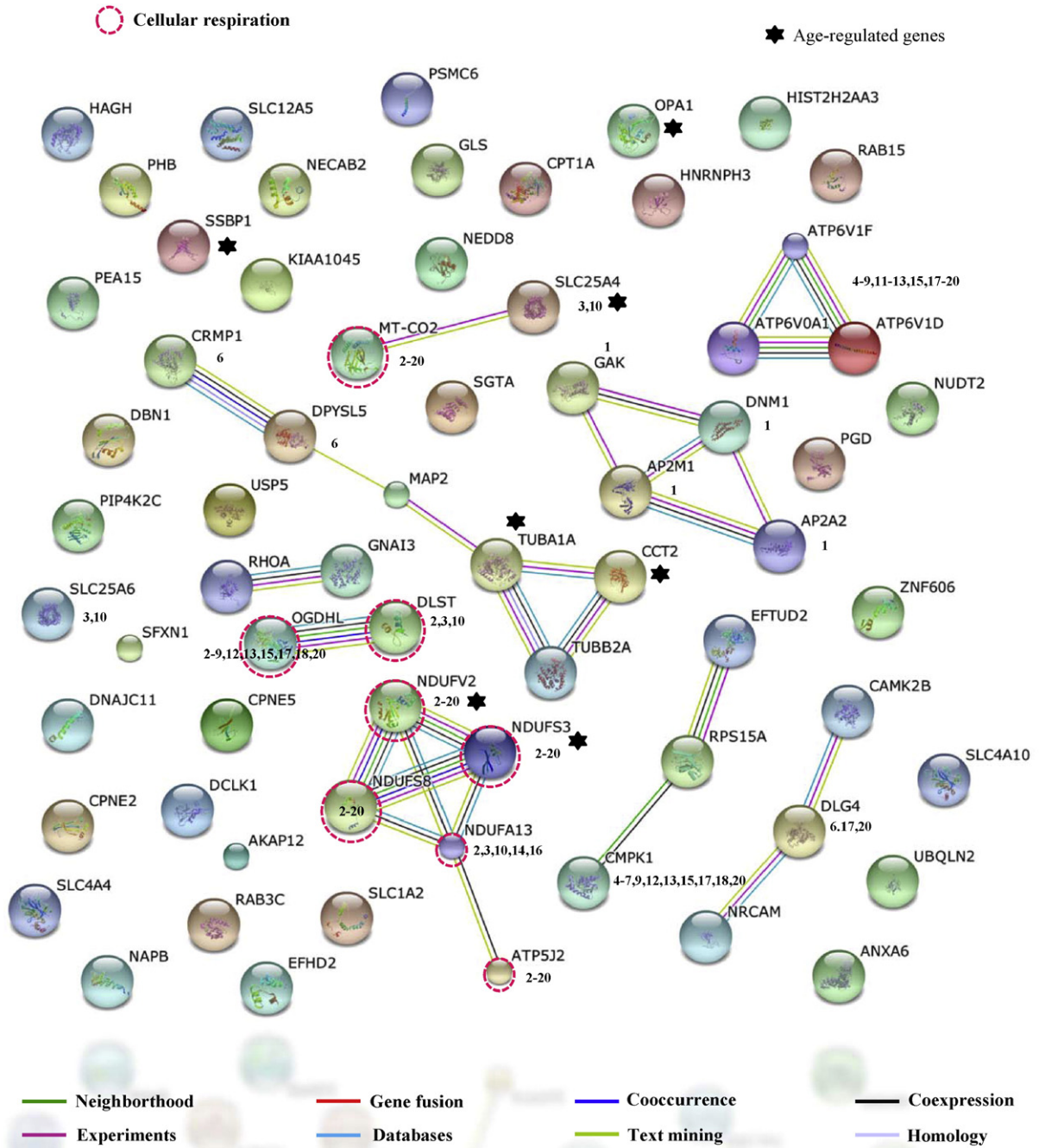
Fig. 4. Interactome of overexpressed polypeptides found consistently in all brains with Alzheimer's disease. UniProtKB accession numbers were submitted to the String program to identify the predicted functional network. Lines in color represent different evidences for each identified interaction. The polypeptides involved in response to stress, response to reactive oxygen species and regulation of inflammatory response were denoted by a pink circle, asterisk and blue circle, respectively. Proteins with bold numbers had a statistical significance (p -Value ≤ 0.05) in the different biological processes that were related. Proteins, whose expression is age-dependent, are labeled with a black star.

diseases, including AD. For this filter, we only obtained two polypeptides as putative biomarkers, APOA1 and CTSD. Finally, we performed an analysis of the filters for the discovery of biomarkers, obtaining two proteins in common for Biomarkers II and III, APOA1 and CTSD (Fig. 7).

3.5. Validation by Western blot of some polypeptides that changed in their expression levels

One polypeptide that was found overexpressed in the MS/MS analysis was ferritin. The Western blot analysis confirmed that it is overexpressed in three Alzheimer's disease brains as well (Fig. 8A). In

the case of Tubulin (Fig. 8C) and Actin (Fig. 8D), two polypeptides that are frequently used as reference in many cell types because their expression levels does not change, they were found subexpressed and overexpressed, respectively, in the three brains with Alzheimer's disease. Other protein assayed by Western blot was the mitochondrial Hsp60 that was found subexpressed in the three AD brains (Fig. 8B). Finally, even though the Tau polypeptide was determined as overexpressed in two AD brains and in the other showed no change (see protein 189, Table 1 in Ref [43]), we tested the expression level by Western blot as it is a key player in Alzheimer's disease. In contrast to our mass spectrometry analysis, we found the Tau polypeptide subexpressed in



- | | |
|--|--|
| 1. Clathrin-mediated endocytosis (4) | 11. ATP metabolic process (6) |
| 2. Cellular respiration (8) | 12. Nucleoside metabolic process (8) |
| 3. Energy derivation by oxidation of organic compounds (10) | 13. Ribonucleotide metabolic process (8) |
| 4. Ribonucleoside monophosphate metabolic process (8) | 14. Electron transport chain (6) |
| 5. Nucleoside monophosphate metabolic process (8) | 15. Ribose phosphate metabolic process (8) |
| 6. Nucleobase-containing small molecule metabolic process (11) | 16. Respiratory electron transport chain (6) |
| 7. Nucleoside triphosphate metabolic process (7) | 17. Nucleoside phosphate metabolic process (9) |
| 8. Purine ribonucleoside monophosphate metabolic process (7) | 18. Glycosyl compound metabolic process (8) |
| 9. Ribonucleoside metabolic process (8) | 19. Purine ribonucleoside triphosphate metabolic process (6) |
| 10. Generation of precursor metabolites and energy (9) | 20. Nucleotide metabolic process (9) |

Fig. 5. Interactome of subexpressed polypeptides found consistently in all brains with Alzheimer's disease. UniProtKB accession numbers were submitted to the String program to identify the predicted functional network. Lines in color represent different evidences for each identified interaction. The polypeptides involved in cellular respiration were denoted by pink circle. Proteins with bold number had a statistical significance (p -Value ≤ 0.05) in the different biological processes that were related. Proteins, whose expression is age-dependent, are labeled with a black star.

Table 3

Classification of the overexpressed and subexpressed proteins found in common in all brains with Alzheimer's disease according to diseases and biofunctions with the IPA software (Core II analysis).

Category	p-Value	N	Molecules
Neurological disease	4.53×10^{-7} to 4.48×10^{-2}	32	FTL , <i>MAP2,PRDX1,GAK,SERPINA3,LDHB,VCAN,SLC12A5,C4A/C4B,CTSD,SLC25A6,SOD2,PREPL,NEDD8,OPA1,DLG4,GFAP,CAMK2B,S100A1,GLS,HNRNPDL,GSN,HP,TUBA1A,NDUFS8,NDUFV2,RTN4,SLC1A2,A2M,SYN2,FTH1,PRDX2</i>
Psychological disorders	1.81×10^{-6} to 4.48×10^{-2}	30	FTL , <i>MAP2,PRDX1,GAK,SERPINA3,VCAN,SLC12A5,LDHB,C4A/C4B,CTSD,SOD2,SLC25A6,PREPL,NEDD8,OPA1,DLG4,GFAP,CAMK2B,S100A1,GLS,GSN,HNRNPDL,TUBA1A,NDUFS8,NDUFV2,RTN4,SLC1A2,SYN2,PRDX2,FTH1</i>
Metabolic disease	2.54×10^{-6} to 9.12×10^{-3}	11	<i>C4A/C4B,CTSD,SOD2,PRDX1,GAK,SLC1A2,OPA1,GFAP,SERPINA3,GSN,CAMK2B</i>
Skeletal and muscular disorders	2.58×10^{-6} to 8.49×10^{-3}	13	FTL , <i>MAP2,SERPINA3,HNRNPDL,VCAN,LDHB,C4A/C4B,SLC25A6,TUBA1A,PREPL,GFAP,FTH1,PRDX2</i>
Cell morphology	1.5×10^{-4} to 4.48×10^{-2}	6	<i>DNM1,SOD2,RHOA,RTN4,OPA1,SYNM</i>
Cell death and survival	1.54×10^{-4} to 4.55×10^{-2}	10	CRYAB , <i>TUBA1A,SIRT2,SOD2,VTN,CAT,SERPINA3,SYNM,PRDX2,FTH1</i>
Hereditary disorder	4.05×10^{-4} to 1.82×10^{-2}	15	S100A1 , <i>MAP2,SERPINA3,GSN,SLC12A5,VCAN,C4A/C4B,SOD2,PREPL,NEDD8,RTN4,SLC1A2,DLG4,GFAP,SYN2</i>
Nervous system development and function	1.68×10^{-3} to 3.6×10^{-2}	3	<i>TUBA1A,RHOA,RTN4</i>
Tissue morphology	1.68×10^{-3} to 9.12×10^{-3}	2	<i>RHOA,RTN4</i>
Cellular compromise	2.23×10^{-3} to 2.23×10^{-3}	2	<i>DNM1,RTN4</i>
Free radical scavenging	4.3×10^{-3} to 9.12×10^{-3}	2	SOD2,PRDX2
Amino acid metabolism	9.12×10^{-3} to 9.12×10^{-3}	1	<i>GLS</i>
Cellular assembly and organization	9.12×10^{-3} to 4.48×10^{-2}	2	<i>OPA1,GFAP</i>
Cellular development	9.12×10^{-3} to 9.12×10^{-3}	1	SIRT2
Cellular growth and proliferation	9.12×10^{-3} to 9.12×10^{-3}	1	SIRT2
Developmental disorder	9.12×10^{-3} to 9.12×10^{-3}	1	GSN
Ophthalmic disease	9.12×10^{-3} to 4.48×10^{-2}	2	SERPINA3,GSN
Small molecule biochemistry	9.12×10^{-3} to 1.82×10^{-2}	3	APOA1,GLS,PRDX2
Behavior	1.82×10^{-2} to 1.82×10^{-2}	1	SOD2
Lipid metabolism	1.82×10^{-2} to 1.82×10^{-2}	1	APOA1
Molecular transport	1.82×10^{-2} to 1.82×10^{-2}	1	APOA1
Cell-to-cell signaling and interaction	3.6×10^{-2} to 3.6×10^{-2}	1	VTN
Organ morphology	3.6×10^{-2} to 3.6×10^{-2}	1	<i>TUBA1A</i>
Tissue development	3.6×10^{-2} to 3.6×10^{-2}	1	VTN
Cancer	4.48×10^{-2} to 4.48×10^{-2}	1	SOD2
Cellular function and maintenance	4.48×10^{-2} to 4.48×10^{-2}	1	SOD2

Proteins in bold correspond to overexpressed proteins.

Proteins in italics correspond to subexpressed proteins.

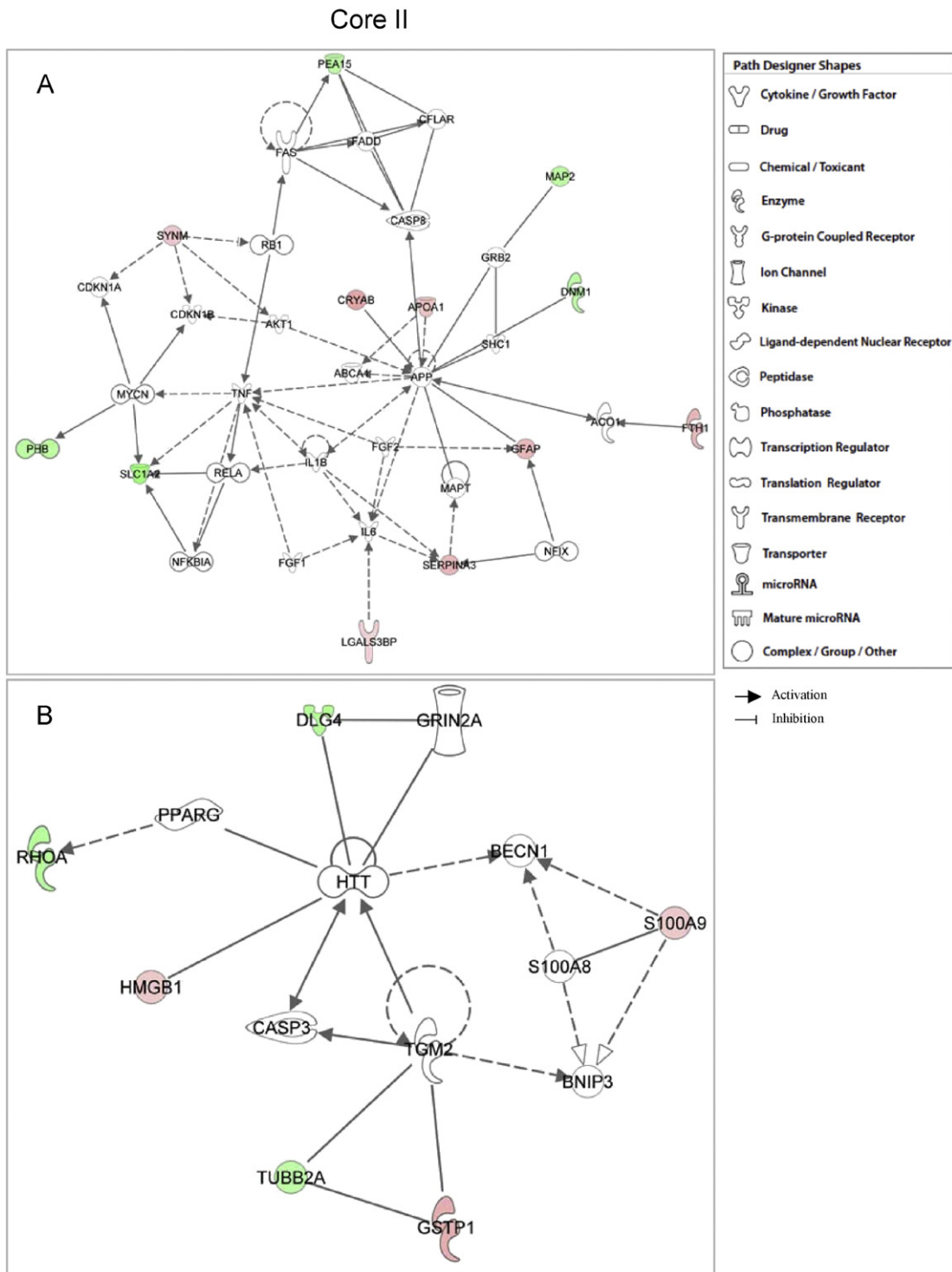


Fig. 6. IPA functional networks of the differentially expressed proteins found in common in all brains with Alzheimer's disease using different core analyses. Core II was associated with: (A) Cell death and survival, free radical scavenging, cellular growth and proliferation, cell morphology, cellular function and maintenance, cellular movement, DNA replication, recombination, and repair; (B) Free radical scavenging, cardiovascular disease, cell death and survival, cancer, and cell morphology. The different forms of the molecules represented are associated with the protein class to which they belong. The proteins in pink and red represent the overexpressed polypeptides and the green molecules correspond to the subexpressed proteins. The gray molecules were proteins incorporated by IPA software because of their relationship with the proteins of interest. The direct relationship between proteins is represented by a continuous line, while indirect relationship by a dotted line. Proteins, whose expression is age-dependent, are labeled with a star (red and blue for over- and sub-expressed, respectively).

the same two AD brains (Fig. 8E). This discrepancy could be explained by the fact that in Alzheimer's disease the Tau polypeptide suffers many posttranslational modifications, including proteolytic

cleavage. All polypeptides corresponding to Tau are expected to be cut by trypsin during sample preparation for MS/MS. In the Western blot analysis we only observed those polypeptides corresponding to

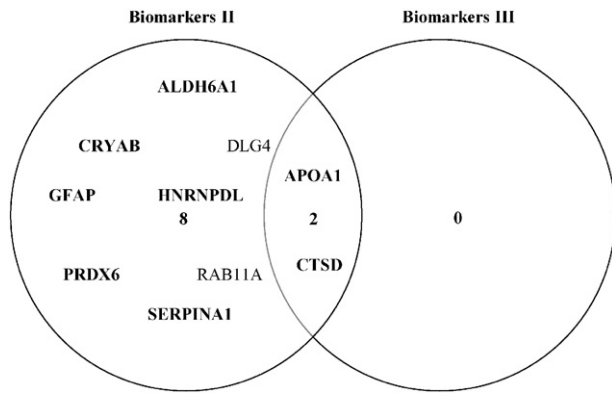


Fig. 7. Venn Euler diagram of candidate proteins to biomarkers found in brains with Alzheimer's disease through the IPA software. The diagram showed two filters of biomarkers. Biomarkers II (tissues and primary cells, including astrocytes and neurons, nervous system, as well as CNS and neuroblastoma cell lines; neurological diseases and psychological disorders), and Biomarkers III (tissues and primary cells, including astrocytes and neurons, nervous system, as well as CNS and neuroblastoma cell lines; Alzheimer as neurological disease). The overexpressed polypeptides are shown in bold letters.

the full-length polypeptide, because the 7.51 mAb is a generic antibody, which recognizes all forms of Tau, excepting PHF that is abundant in the highly insoluble NFTs [44].

3.6. *In vivo* validation of selected candidates

To validate the potential involvement of selected candidate hits in A β or Tau pathologies, we capitalized on the *Drosophila* eye phenotypes elicited by human A β 42 and Tau. Fig. 9 (E and I) shows that the expression of A β 42 and Tau induced a glassy eye and disrupted the highly ordered lattice of the ommatidia when compared to control flies expressing a LacZ transgene (Fig. 9A). As proof of principle for the validation, we selected three proteins for which there is little or no information regarding their involvement in AD: RhoA/Rho1, Sideroflexin, and Phosphoglucomutase 1 (PGM1). We first tested a dsRNA transgene against Rho1 in the context of the *gmr-Gal4* driver alone and found no modification of the eye morphology (Fig. 9B). However, the Rho1 RNAi construct induced a very aggressive phenotype in A β 42- and Tau-expressing flies (Fig. 9, F and J). Notably, we observed similar necrotic patterns in both models, suggesting that Rho1 may interact genetically with a common pathological pathway mediated by A β 42 and Tau. We then tested a heterozygous *P*-element insertion that disrupts the mitochondrial domain of the Sideroflexin orthologue, referred to as CG11739^{d0683} (Fig. 9C). We found that reducing the function of fly Sideroflexin does not modify the A β 42-induced phenotype (compare Fig. 9E and G). However, it dramatically reduced the size of the eye in Tau-expressing flies (Fig. 9I and K). This distinct result suggests that Sideroflexin is specifically involved in Tau-mediated toxicity. Finally, we tested an RNAi construct against Phosphoglucomutase-1 (PGM1) and found no phenotype when crossed with the *gmr-Gal4* driver alone (Fig. 9D). In contrast, flies coexpressing the A β 42 and PGM1 RNAi transgenes exhibited a dramatic induction of necrotic dots throughout the external lens when compared to A β 42 only flies (Fig. 9, E and H, arrowheads). Interestingly, no apparent modification of the Tau phenotype was observed when the PGM1 RNAi construct was tested (Fig. 9, I and L). In this regard, the absence of necrotic dots supports the specificity of the interaction between A β 42 and PGM1. Taken together, these results validate some of the proteins identified by proteomics and highlight the power of *Drosophila* genetics to identify molecules that can specifically interact with A β 42, Tau or both. Thus, a separate study will be performed to validate the rest of the hits in this experimental system.

4. Discussion

We have previously reported the identification of > 100 polypeptides in whole homogenates and isolated NFTs from fixed human Alzheimer's brain tissues [31]. Some of these proteins have already been reported by other researchers, including GADPH, which has been linked to AD as a possible biomarker, UCHL-1, related to oxidative stress, and Transferrin, identified as an iron regulatory protein [31]. However, the identification was only qualitative. Therefore, in this work we report the identification of 721 polypeptides through a quantitative proteomic analysis of three different AD brains and one more used as a control, thus expanding the number of proteins corresponding to the proteome of AD brains (Table 1 in [43]). The number of overexpressed polypeptides was 61, which corresponds to 8.5% of the total identified polypeptides (Table 1), while the subexpressed proteins were 69 (Table 2), representing the 9.6% of the total. Tau is one of the key proteins involved in AD that was not identified in our previous work [45]. However, Tau was detected and quantified in this report (Table 1 in [43]; Figs. 1 and 10).

Overexpressed polypeptides were grouped in five main protein classes, including oxidoreductases, defense immunity, enzyme modulators, hydrolases, and signaling molecules (Fig. 3). Some proteins may be part of different classes and therefore be involved in different biological processes (Fig. 3 and Fig. 4). However, some of them constitute two main interaction networks as revealed by String program (Fig. 4). The first one is related to stress, and included the genes *SERPINA1*, *HP*, *HBA1*, *A2M*, *APOA1*, *APCS*, *GSN*, *ACTA1*, *HSPB1* and *HMGB1*. Inasmuch as *A2M*, *HBA1* and *HSPB1* are genes whose expression was found to be dependent on age, they were not further considered in the present study. The *SERPINA1* gene encodes the α -1-antitrypsin, which belongs to the superfamily of serpins or serine proteinase inhibitors. We found it overexpressed in the AD brains, with values ranging between 26% and 184% (Table 1), and it has been proposed as a putative biomarker in brain amyloid burden [45] and Alzheimer's disease as well [46]. Albeit *SERPINA3* (Table 1 and Fig. 4), which encodes the α -1-antichymotrypsin, is not included in the node of *SERPINA1*, its gene product has been localized in fibrillar amyloid- β plaques [47]. A potential role in AD has been spotlighted by the finding that a polymorphism in the *SERPINA3* gene promoter has been associated with longer survival of patients with Alzheimer's disease [48]. However, its functions remain to be determined.

In relation to Haptoglobin, encoded by the *HP* gene, it has been described as a potent antioxidant molecule that strongly interacts with the *HBA1* gene product, the Hemoglobin, protecting it from redox inactivation [49]. The expression levels found in the present work ranged between 42% and 258% in the AD brains studied (Table 1). Moreover, Haptoglobin, which is related to the acute-phase of inflammation [50], has been described as a molecule that binds ApoA-I as well (reported in our work as overexpressed, with values between 16 and 60%, see Table 1), which is the principal component of the high-density lipoprotein (HDL) involved in the reverse cholesterol transport removal [51]. Remarkably, Haptoglobin is able to interact with two key players in AD, Apolipoprotein E and Amyloid- β [50], and has been proposed as a putative biomarker to be detected in CSF, together with Tau, in order to discriminate individuals with Alzheimer's disease and those with other dementias [52]. Moreover, Haptoglobin has been detected as subexpressed or highly oxidized in serum of patients with Alzheimer's disease and those with mild cognitive impairment [53]. However, we detected it as overexpressed in AD brains (Table 1).

Finally, the gene product of *APCS*, the serum Amyloid P component or SAP, has been found associated to deposits of amyloid [54], including those produced in Alzheimer's disease [55]. It is produced by pyramidal neurons in hippocampus [55], binds to fibrils of amyloid- β deposits in a Ca⁺²-dependent manner, and is able to inhibit the formation of amyloid- β deposits *in vitro* [56]. SAP has been found expressed at reduced levels in individuals that show the Alzheimer's disease pathology

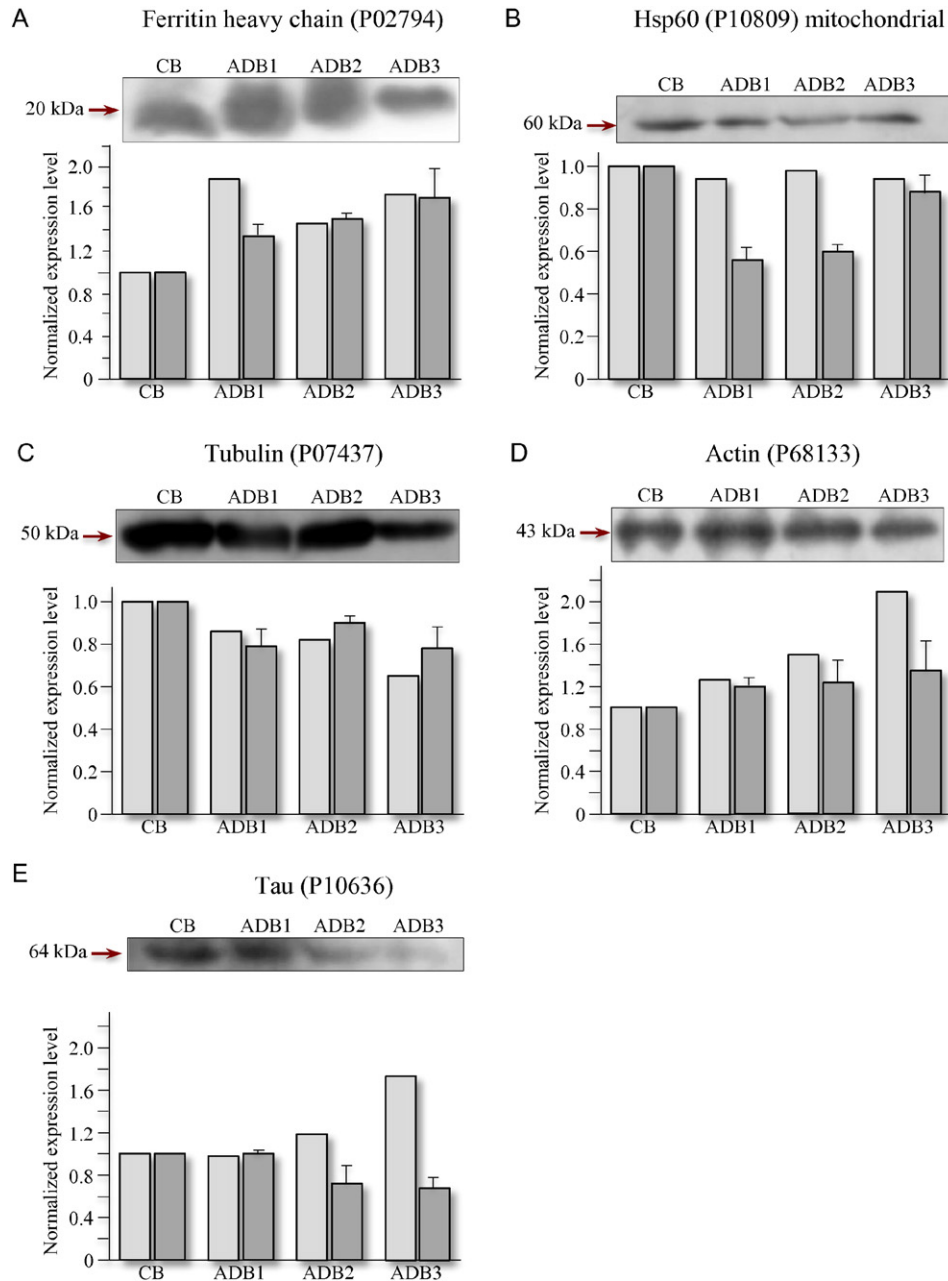


Fig. 8. Validation of some polypeptides by western blot using whole tissue extracts from brains with Alzheimer's disease. Western blots and densitometry analyses of the overexpressed heavy chain of Ferritin (A) and subexpressed Hsp60 (B) polypeptides. We also analyzed Tubulin (C), Actin (D) and Tau (E). Densitometry values were normalized to the loading control brain. Light boxes, values obtained in MS/MS analysis. Dark boxes, values obtained in Western blot analysis. Bars correspond to standard deviation.

but lacking dementia [57]. Interestingly, we found it overexpressed in AD brains, with relative values varying between 36% and 414% (Table 1). All these observations have pointed on SAP as a putative target in Alzheimer's disease. Accordingly, the use of the (R)-1-(6-((R)-2-carboxy-pyrrolidin-1-yl)-6-oxo-hexanoyl) pyrrolidine-2-carboxylic acid (CPHPC) compound depleted SAP in sera and greatly reduced its expression level in CSF from patients with mild to moderate Alzheimer's disease [58].

The second network comprises the genes *FTL*, *FTH1*, *CAT*, *SOD2*, *PRDX1*, *PRDX2*, *PRDX6*, *GSTP1*, and *GSTM1*, which are all involved in oxidation-reduction reactions (Fig. 4). The Ferritin is a large supramolecular structure of 450 kDa, formed by 24 subunits. It has a storage capacity of 4500 atoms of iron. In addition, it has a ferroxidase catalytic site in the heavy chain, encoded by the *FTH1* gene, which oxidizes Fe^{2+} to Fe^{3+} . Even though the *FTL* gene product (the Ferritin light chain) lacks the catalytic site, it contains a higher number of carboxyl

groups than heavy chain in the cavity of the supramacromolecular structure, which is utilized to nucleate iron. Moreover, Ferritin in serum is found increased during chronic and acute inflammation [59, 60], and is produced by microglia, among other cells [61]. In the AD brains in this study, both chains of Ferritin were found overexpressed, with values ranging from 46% to 88%, and 37% to 165% for the heavy and light chains, respectively. However, more studies are required to use it as a putative biomarker since Ferritin has also been found overexpressed in a number of cancers [60].

The other proteins in the network are Catalase, mitochondrial Superoxide dismutase, Peroxiredoxin-1, -2 and -6, Glutathione-S-transferase Pi 1 and Glutathione-S-transferase Mu 1. All of these enzymes protect cells from the deleterious effects produced by ROS [61]. Catalase is widely distributed in nearly all the organisms that are exposed to oxygen and is responsible for the oxidation of H_2O_2 to molecular oxygen and water. It has been involved in several biological

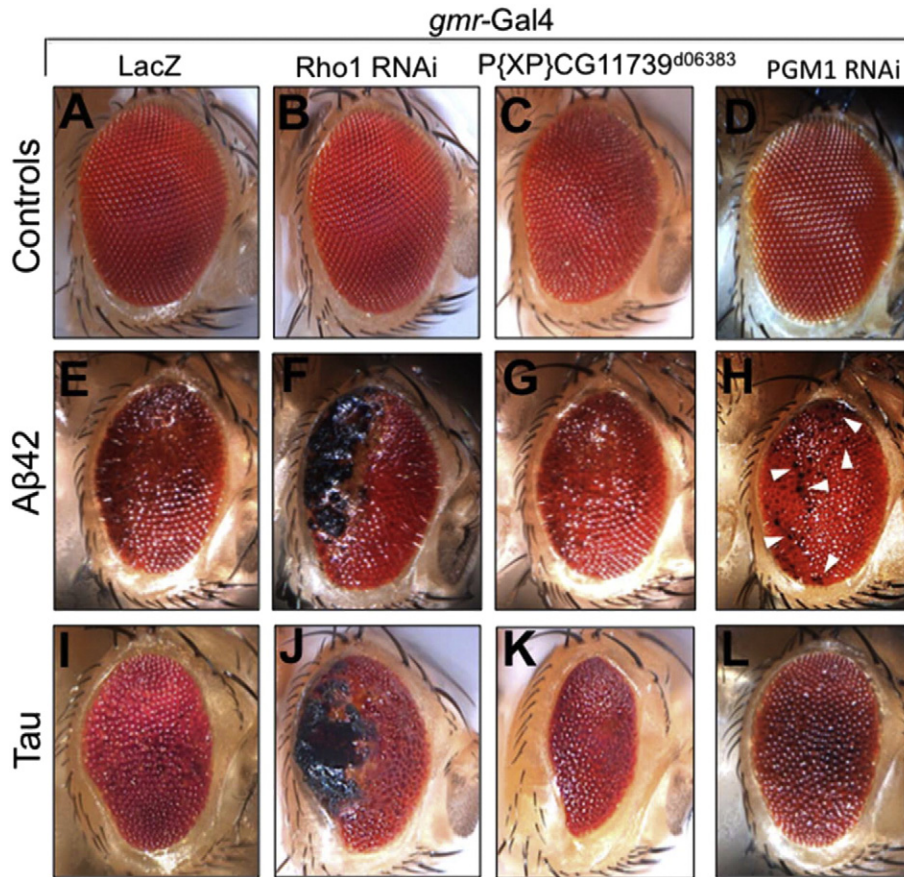


Fig. 9. In vivo validation of selected hits in fly models of A β 42- and Tau-induced toxicity. Images show fresh eyes from flies expressing control transgenes alone (A–D) or in the context of human A β 42 (E–H) and Tau (I–L) transgenes via the UAS/Gal4 system (*gmr-Gal4*) at 26 °C. Note that flies from control crosses (A–D) do not display major morphological abnormalities. However, silencing of Rho1 enhances the eye phenotypes of both A β 42- and Tau-expressing flies (E and I) and induces similar posterior necrotic spots (F and J). In addition, reduction of Sideroflexin function exacerbates Tau (see smaller eye in K) but not A β 42 (G) toxicity. Conversely, silencing of PGM1 exacerbates A β 42 (H) but not Tau (L) phenotypes. Arrowheads in H point to necrotic dots.

processes including apoptosis prevention, inflammation, and stimulation of tumorigenesis [62]. The catalase expression levels found varied from 17% to 119% in the AD brains (Table 1). Noteworthy, A β 42 can bind catalase and inhibit its enzymatic activity [63] and therefore could favor the generation of ROS. Albeit this interaction could be detrimental it also could be beneficial as it inhibits the aggregation process of amyloid- β [64]. Other report suggests that inhibition of A β -catalase interaction might guard SH-SY5Y neuroblastoma cells from toxicity and oxidative stress produced by A β [65].

In the case of Peroxiredoxin-1, -2 and -6, they were found overexpressed in AD brains, ranging between 15% and 84% (Table 1), and might be reflecting an increase in the oxidative stress present in Alzheimer's disease brains. Peroxiredoxins are considered as oxidative stress biomarkers, as they are part of the defense machinery against H₂O₂ and have emerging key roles in the antioxidant system as well, for example as redox sensors [66]. They are very sensitive to hyperoxidation and inactivation, and are also considered as gerontogenes, because they have been linked to genome stability and signaling pathways that are responsive to nutrients as a function of age [67]. The lack of the *Prdx1* gene caused a significant reduction in the lifespan of the *Prdx1*^{-/-} mouse, hemolytic anemia and several cancers, as a consequence of increased ROS, supporting a role as a tumor suppressor and as antioxidant [68]. In *Saccharomyces cerevisiae*, the lack of Tsa1, the major yeast peroxiredoxin, causes an increase in mutation rates and genome instability [68,69], and extension of lifespan as well [70]. Noteworthy, Tsa1 has been recently involved in a protective role in the oxidative stress produced by the misfolding of nascent polypeptides and protein aggregation [71].

The mitochondrial Superoxide dismutase 2 (SOD2) is responsible for the conversion of superoxide anion into H₂O₂, reducing in this way the potential risk of reaction of O₂ with macromolecules [72]. It has been found overexpressed at mRNA level in lymphocytes from patients with AD [73]. The key role of SOD2 in AD has been spotlighted with AD mice models, where a deficiency in this enzyme causes an increase in the formation of amyloid- β deposits and Tau phosphorylation. On the contrary, an increase in the SOD2 levels produced a diminishing of the Amyloid- β 42/Amyloid- β 40 ratio, which is considered a condition not favorable for the formation of amyloid- β plaques [74]. In other work, it was found with no changes in its expression level in the *APP^{NLh/NLh} PS1^{P264L/P264L}* double knock-in AD mouse model, although there was observed SOD2 nitration that negatively affected its enzymatic activity and impairment of mitochondrial function [75].

Finally, the Glutathione-S-transferases Pi1 (GSTP1) and Mu1 (GSTM1) are enzymes that belong to the family of GSTs, involved in the Phase II detoxification system whose main function is conjugate reduced glutathione to a number of electrophilic compounds and products of the oxidative stress [76]. GSTs have been involved in cell growth and progression of some diseases [77], and are regulated by the transcription factor Nrf2, a master gene that regulates the expression of a number of genes involved in the defense against ROS and reactive nitrogen species (RNS) [78]. GSTP1 negatively regulates the activity of JNK through protein-protein interactions. JNK is a stress kinase that is transiently activated in response to ROS/RNS, heat shock, osmotic shock, growth factors or inflammatory cytokines [78]. Remarkably, GSTP1 interacts with Cdk5 and inhibits its kinase activity through protein-protein interactions, in a ROS-dependent manner [79]. GSTM1 can

bind ASK1, a MAPKKK that also activates JNK and the p38 pathways through protein-protein interactions, in a similar way as GSTP1 [80]. GSTP1 was found overexpressed, with values ranging between 35% and 97%, while GTSM1 varied between 40% and 110% in the AD brains (Table 1).

In relation to the subexpressed polypeptides, we found several proteins that belong to different complexes of the respiratory chain (Fig. 5). The NADH dehydrogenase complex I was the main complex of the respiratory chain which showed more affected subunits: NDUFS3, NDUFS8, NDUFV2 and NDUFA13, whose relative values diminished from 18% to 24%, 15% to 62%, 22% to 43%, and 39% to 51% in the AD brains, respectively (Table 2). Even though the expression levels of NDUFS3 and NDUFV2 are age-dependent, they should be considered as molecules involved in AD since one of the main risk factors of sporadic cases of Alzheimer's disease is age, as well as all the other proteins identified with the same characteristic. The other affected complexes in the mitochondria were the Cytochrome c oxidase (complex IV) and the ATP synthase (complex V), each with only one protein, the Cytochrome c oxidase subunit 2 (COX2) and the ATP synthase subunit f (ATP5J2). In addition, we found subexpressed the ADP/ATP translocases 1 (SLC25A4) and 3 (SLC25A6), which are responsible of the exchange of ADP/ATP across the inner membrane of mitochondria and are proapoptotic molecules [81]. Even though the expression of SLC25A4 is age-dependent [38], it might also have a key role in AD.

The oxidative stress and mitochondrial dysfunction have already been related to aging and Alzheimer's disease. At advanced ages, production rates of ATP and NAD⁺ could be low in neurons, causing impaired mitochondrial function. Defects in only one complex or complex subunit may lead to several respiratory chain defects [82]. Remarkably, the complex I is quite sensitive to oxidative damage, because it has iron-sulfur clusters, which can be attacked by ROS/RNS. This complex has seven subunits that are encoded in the mitochondrial DNA (mtDNA), and their subunits are more susceptible to mtDNA mutations caused by ROS [83–85]. Deficiencies in the subunits of 24 kDa, 25 kDa and 30 kDa of complex I have been reported in Parkinson's disease [86]. In the case of the 24 kDa and 75 kDa subunits of complex I, they were found at reduced levels in patients with AD, as well as in patients with Down syndrome [87]. The importance of this complex is spotlighted by the fact that the reductions of some subunits might contribute to deficiency of energy metabolism and result in neuronal apoptosis [88]. Finally, the activity of cytochrome c oxidase (COX) was found reduced in platelets and hippocampus from the AD patients [89].

Other machinery that seems to be affected is the vacuolar ATPase (V-ATPase). This molecule has as main role de acidification of eukaryotic organelles. However, other roles have been discovered in the last years for V-ATPase, including regulation of transduction pathways, the endocytic and exocytic pathways, and as pH sensor and receptor for the cytohesin-2/Arf-family GTP-binding proteins [90]. The V-ATPase subunits that were found subexpressed in the AD brains were the V1-subunit D (ATP6V1D), V1-subunit F (ATP6V1F) and the V0-subunit a (ATP6VOA1) (Fig. 5), varying their expression levels between 15% to 37%, 17% to 49%, and 15% to 30%, respectively (Table 2).

Proteins not included in any of the interactomes also have key roles in cellular function. For example, the transforming protein RhoA was found subexpressed in the three AD brains, showing a reduction in its expression levels between 27% and 31% (Table 2). RhoA regulates a signal transduction pathway that is involved in the regulation of several neuronal functions including development of dendrites, extension of axon and migration [91], and has a key role in the stabilization of microtubules induced by A β in NIH3T3 cells, which was disrupted when RhoA was inhibited [92]. Thus, the reduction in the neuronal connections observed in the AD brains might be explained by the loss of synaptic connections mediated by a decrease in the amount of RhoA.

Another protein that was subexpressed in the AD brains is Sideroflexin-1 (SFXN1). The function of this protein in vivo remains unknown. Early studies indicated that Sideroflexin 3 was the orthologous of

the rat citrate transport protein and as all members of the family in human have five transmembrane domains which remembers the structure of mitochondrial anion transporters [93]. Both Sideroflexin-1 and -3 are both targeted to mitochondria and all members of the Sideroflexin family are expressed in rat pancreatic islets [93,94]. Sideroflexin-1 was found subexpressed in all AD brains, showing a reduction from 17% to 53% (Table 2). The role of Sideroflexin-1 in Alzheimer's disease is an issue that remains unveiled.

DLG4 (Disk large homolog 4, previously known as PSD95) and excitatory amino acid transporter 2 (GLT-1 or SLC1A2) are two proteins expressed in both post- and pre-synapses, which showed decreased expression levels in the present study. Recent works suggest that these two proteins have relation with AD. Thus, PSD95 is a major element of synapses and involved in aging processes and has been found to have a direct relation with the distribution of A β . In addition, PSD-95 decreased is associated with deficient synaptic plasticity. Meanwhile, GLT-1 a glutamate transporter in the in the cerebral cortex and hippocampus, has an important role regulating extracellular glutamate levels. Therefore, functional loss of GLT-1 has been reported to correlate well with synaptic degeneration and severity of cognitive impairment. All previous studies suggest that DLG4 and GLT-1 restoration could be neuroprotective and might help reducing pathogenic processes associated with AD [95–103].

Proteins identified in our study belong to biological processes that are similar to those found in different proteomics studies using different tissues sections, including those carried out with olfactory bulb [101], and in the CA and dentate gyrus of hippocampus of patients with AD [102], revealing functional similarities in all studied brains with AD.

5. Conclusions

We have identified several proteins that changed in their expression level in brains with Alzheimer's disease. Albeit their cellular functions are diverse, two features clearly emerge in this disease: 1) The normal function of mitochondrion is severely affected, and 2) there is an alteration of expression levels of proteins involved in ROS. Thus, our data supports the general overview of this disease. In addition, we provide evidence on the use of *Drosophila melanogaster* as an in vivo model to determine the effects of novel proteins on the function of key players in AD, such as Amyloid- β and Tau.

Acknowledgements

We thank Conacyt from Mexico for the financial support of this project to Raul Mena and Juan Pedro Luna-Arias, as well as for a Ph.D. scholarship and a postdoctoral fellowship to Benito Minjarez. We are also grateful for a postdoctoral fellowship from ICyTDF from Mexico, now renamed SECITI, to María Esther Herrera-Aguirre. In addition, we thank the McKnight Brain Institute at the University of Florida for a Research Development Award to Diego E. Rincon-Limas. We also thank Claude M. Wischik, Charles R. Harrington and Manuel Hernandez for sharing antibodies, Matt Mahoney for the Tau flies, and the Bloomington Stock Center for fly strains. Finally, we thank all donor families for their support.

References

- [1] Dementia: A public health priority. World Health Organization and Alzheimer's Disease International, World Health Organization Report. (2012) <http://www.who.int>.
- [2] Alzheimer's Association. Alzheimer's Disease Facts and Figures, *Alzheimers Dement.* (2012) 8(2).
- [3] H. Braak, E. Braak, Neuropathological staging of Alzheimer-related changes, *Acta Neuropathol. (Berl.)* 82 (1991) 239–259.
- [4] P.T. Nelson, H. Braak, W.R. Markesbery, Neuropathology and cognitive impairment in Alzheimer disease: A complex but coherent relationship, *J. Neuropathol. Exp. Neurol.* 68 (2009) 1–14.
- [5] R.E. Tanzi, The genetics of Alzheimer Disease, *Cold Spring Harb Perspect Med* 2 (2012) a006296.

- [6] S. Weintraub, A.H. Wicklund, D.P. Salmon, The neuropsychological profile of Alzheimer disease, *Cold Spring Harb Perspect Med* 2 (2012) a006171.
- [7] Klein WL. Cytotoxic intermediates in the fibrillation pathway: A β oligomers in Alzheimer's disease as a case study. In: Uvertsky VN, Fink AL, editors. *Protein Misfolding, Aggregation, and Conformational Diseases. Part A: Protein Aggregation and Conformational Diseases*. Springer, New York; 2006. p. 61–75.
- [8] M. Hüll, M. Berger, M. Heneka, Disease-modifying therapies in Alzheimer's disease: how far have we come? *Drugs* 66 (2006) 2075–2093.
- [9] C.M. Wischik, R.A. Crowther, S. Murray, M. Roth, Subunit structure of paired helical filaments in Alzheimer's disease, *Nature* 100 (1985) 1905–1912.
- [10] K.S. Kosik, C.L. Joachim, D.J. Selkoe, Microtubule associated protein tau (τ) is a major antigenic component of paired helical filaments in Alzheimer disease, *Proc. Natl. Acad. Sci. U. S. A.* 83 (1986) 4044–4048.
- [11] I. Grundke-Iqbal, K. Iqbal, Y.C. Tung, M. Quinlan, H.M. Wisniewski, L.I. Binder, Abnormal phosphorylation of the microtubule-associated protein tau (τ) in Alzheimer cytoskeletal pathology, *Proc. Natl. Acad. Sci. U. S. A.* 83 (1986) 4913–4917.
- [12] I. Grundke-Iqbal, K. Iqbal, M. Quinlan, Y.C. Tung, M.S. Zaidi, H.M. Wisniewski, (1986) Microtubule-associated protein tau. A component of Alzheimer paired helical filaments, *J. Biol. Chem.* 261 (1986) 6084–6089.
- [13] M.A. Korhonen, T.A. Nyman, T. Aittokallio, T. Pirttilä, An update on clinical proteomics in Alzheimer's research, *J. Neurochem.* 112 (2010) 1386–1414.
- [14] T.A. Clark, H.P. Lee, R.K. Rolston, X. Zhu, M.W. Marlett, R.J. Castellani, et al., Oxidative stress and its implications for future treatments and management of Alzheimer Disease, *Int. J. Biomed. Sci.* 6 (2010) 225–227.
- [15] P. Coskun, J. Wyrembak, S. Schriener, H.W. Chen, C. Marciniak, F. LaFerla, D.C. Wallace, A mitochondrial etiology of Alzheimer and Parkinson disease, *Biochim. Biophys. Acta* 2013 (1820) 553–564.
- [16] A. Abeti, M.R. Duchon, Activation of PARP by oxidative stress induced by amyloid: Implications for Alzheimer's Disease, *Neurochem. Res.* 37 (2012) 2589–2596.
- [17] V. Cavallucci, M. D'Amelio, F. Cecconi, A β toxicity in Alzheimer's Disease, *Mol. Neurobiol.* 45 (2012) 366–378.
- [18] R. Kaye, C.A. Lasagna-Reeves, Molecular mechanisms of amyloid oligomers toxicity, *J. Alzheimers Dis.* 33 (2013) S67–S78.
- [19] T. Tomita, T. Iwatsubo, Structural biology of presenilins and signal peptide peptidases, *J. Biol. Chem.* 288 (2013) 14673–14680.
- [20] I. Belinova, E. Karan, B. De Strooper, The toxic A β oligomer and Alzheimer's disease: an emperor in need of clothes, *Nat. Neurosci.* 15 (2012) 349–357.
- [21] C.X. Gong, F. Liu, I. Grundke-Iqbal, K. Iqbal, Post-translational modifications of tau protein in Alzheimer's disease, *J. Neural Transm.* 112 (2005) 813–838.
- [22] J. Luna-Muñoz, L. Chávez-Macías, F. García-Sierra, R. Mena, Earliest stages of tau conformational changes are related to the appearance of a sequence of specific phospho-dependent tau epitopes in Alzheimer's disease, *J. Alzheimers Dis.* 12 (2007) 365–375.
- [23] F. García-Sierra, N. Ghoshal, B. Quinn, R.W. Berry, L.I. Binder, Conformational changes and truncation of tau protein during tangle evolution in Alzheimer's disease, *J. Alzheimers Dis.* 5 (2003) 65–77.
- [24] M. Gorath, T. Stahnke, T. Mronga, O. Goldbaum, C. Richter-Landsberg, Developmental changes of tau protein and mRNA in cultured rat brain oligodendrocytes, *Glia* 36 (2001) 89–101.
- [25] W.H. Stoothoff, G.V.W. Johnson, Tau phosphorylation: physiological and pathological consequences, *Biochim. Biophys. Acta* 2005 (1739) 280–297.
- [26] S.M. Greenberg, E.H. Koo, D.J. Selkoe, W.Q. Qiu, K.S. Kosik, Secreted beta-amyloid precursor protein stimulates mitogen-activated protein kinase and enhances tau phosphorylation, *Proc. Natl. Acad. Sci. U. S. A.* 91 (1994) 7104–7108.
- [27] D.P. Hanger, B.H. Anderton, W. Noble, Tau phosphorylation: the therapeutic challenge for neurodegenerative disease, *Trends Mol. Med.* 15 (2009) 112–119.
- [28] J.Z. Wang, Y.Y. Xia, I. Grundke-Iqbal, K. Iqbal, Abnormal hyperphosphorylation of tau: sites, regulation, and molecular mechanism of neurofibrillary degeneration, *J. Alzheimers Dis.* 1 (2013) S123–S139 33Suppl.
- [29] G.E. Craft, A. Chen, A.C. Nairn, Recent advances in quantitative neuroproteomics, *Methods* 61 (2013) 186–218.
- [30] J.R. Yates, C.I. Ruse, A. Nakorchevsky, Proteomics by mass spectrometry: approaches, advances, and applications, *Annu. Rev. Biomed. Eng.* 11 (2009) 49–79.
- [31] B. Minjarez, M.L. Valero Rustarazo, M.M. Sanchez del Pino, A. González-Robles, J.A. Sosa-Melgarejo, J. Luna-Muñoz, et al., Identification of polypeptides in neurofibrillary tangles and total homogenates of brains with Alzheimer's disease by tandem mass spectrometry, *J. Alzheimers Dis.* 34 (2013) 239–262.
- [32] S. Chen, F.F. Lu, P. Seeman, F. Liu, Quantitative proteomic analysis of human substantia nigra in Alzheimer's disease, Huntington's disease and multiple sclerosis, *Neurochem. Res.* 37 (2012) 2805–2813.
- [33] P. Rudrabhatla, P. Grant, H. Jaffe, M.J. Strong, H.C. Pant, Quantitative phosphoproteomic analysis of neuronal intermediate filament proteins (NF-M/H) in Alzheimer's disease by iTRAQ, *FASEB J.* 24 (2010) 4396–4407.
- [34] Y.V. Skorobogatko, J. Deuso, J. Adolf-Bergfoyle, M.G. Nowak, Y. Gong, C.F. Lipka, K. Vosseller, Human Alzheimer's disease synaptic O-GlcNAc site mapping and iTRAQ expression proteomics with ion trap mass spectrometry, *Amino Acids* 40 (2011) 765–779.
- [35] F. Abdi, J.F. Quinn, J. Jankovic, M. McIntosh, J.B. Leverenz, E. Peskind, et al., Detection of biomarkers with a multiplex quantitative proteomic platform in cerebrospinal fluid of patients with neurodegenerative disorders, *J. Alzheimers Dis.* 9 (2006) 293–348.
- [36] B. Martin, R. Brenneman, K.G. Becker, M. Gucek, R.N. Cole, S. Maudsley, iTRAQ analysis of complex proteome alterations in 3xTgAD Alzheimer's mice: understanding the interface between physiology and disease, *PLoS One* 3 (2008), e2750.
- [37] V. Rhein, X. Song, A. Wiesner, L.M. Ittner, G. Baysang, F. Meier, et al., Amyloid-beta and tau synergistically impair the oxidative phosphorylation system in triple transgenic Alzheimer's disease mice, *Proc. Natl. Acad. Sci. U. S. A.* 106 (2009) 20057–20062.
- [38] M. Melé, P.G. Ferreira, F. Reverter, D.S. DeLuca, J. Monlong, M. Sammeth, et al., Human genomics. The human transcriptome across tissues and individuals, *Science* 348 (2015) 660–665.
- [39] G. McKhann, D. Drachman, M. Folstein, R. Katzman, D. Price, E.M. Stadlan, Clinical diagnosis of Alzheimer's disease: report of the NINCDS-ADRDA Work Group under the auspices of Department of Health and Human Services Task Force on Alzheimer's Disease, *Neurology* 34 (1984) 939–944.
- [40] M.M. Bradford, A rapid and sensitive for the quantitation of microgram quantities of protein utilizing the principle of protein-dye binding, *Anal. Biochem.* 72 (1976) 248–254.
- [41] H. Mi, A. Muruganujan, P.D. Thomas, PANTHER in 2013: modeling the evolution of gene function, and other gene attributes, in the context of phylogenetic trees, *Nucl Acids Res* 41 (2013) D377–D386.
- [42] S. Casas-Tinto, Y. Zhang, J. Sanchez-García, M. Gomez-Velazquez, D.E. Rincon-Limas, P. Fernandez-Funez, The ER stress factor XBP1s prevents amyloid-beta neurotoxicity, *Hum. Mol. Genet.* 20 (2011) 2144–2160.
- [43] Minjarez B, Calderón-González KG, Valero-Rustarazo ML, Herrera-Aguirre ME, Labra-Barrios ML, Rincon-Limas DE, et al. Data set of identification of proteins that are differentially expressed in brains with Alzheimer's disease using iTRAQ labeling and tandem mass spectrometry. Data in Brief (submitted).
- [44] M. Novak, R. Jakes, P.C. Edwards, C. Milstein, C.M. Wischick, Differences between the tau protein of Alzheimer paired helical filament core and normal tau revealed by epitope analysis of monoclonal antibodies 423 and 7.51, *Proc. Natl. Acad. Sci. U. S. A.* 88 (1991) 5837–5841.
- [45] S.J. Kiddle, M. Thambisetty, A. Simmons, J. Riddoch-Contreras, A. Hye, E. Westman, et al., Plasma based markers of [11C] PiB-PET brain amyloid burden, *PLoS One* 7 (2012), e44260.
- [46] S.J. Kiddle, M. Sattler, P. Proitsi, A. Simmons, E. Westman, C. Bazenet, et al., Candidate blood proteome markers of Alzheimer's disease onset and progression: a systematic review and replication study, *J. Alzheimers Dis.* 38 (2014) 515–531.
- [47] C.R. Abraham, D.J. Selkoe, H. Potter, Immunochemical identification of the serine protease inhibitor α 1-antichymotrypsin in the brain amyloid deposits of Alzheimer's disease, *Cell* 52 (1998) 487–501.
- [48] F. Licastro, M. Chiappelli, L.J. Thal, E. Masliah, Alpha-1-Antichymotrypsin polymorphism in the gene promoter region affects survival and synapsis loss in Alzheimer's disease, *Arch. Gerontol. Geriatr. Suppl.* 9 (2004) 243–251.
- [49] A.I. Alayash, Haptoglobin: old protein with new functions, *Clin. Chim. Acta* 412 (2011) 493–498.
- [50] M.S. Spagnuolo, B. Maresca, V. La Marca, A. Carrizzo, C. Veronesi, C. Cupidi, et al., Haptoglobin interacts with apolipoprotein E and beta-amyloid and influences their crosstalk, *ACS Chem. Neurosci.* 5 (2014) 837–847.
- [51] L. Cigliano, C.R. Pugliese, M.S. Spagnuolo, R. Palumbo, P. Abrescia, Haptoglobin binds the antiatherogenic protein apolipoprotein E - impairment of apolipoprotein E stimulation of both lecithin: cholesterol acyltransferase activity and cholesterol uptake by hepatocytes, *FEBS J* 276 (2009) 6158–6171.
- [52] J.D. Abraham, S. Calvayrac-Pawlowski, S. Cobo, N. Salvétat, G. Vicat, M. Molina, et al., Combined measurement of PEDF, haptoglobin and tau in cerebrospinal fluid improves the diagnostic discrimination between Alzheimer's disease and other dementias, *Biomarkers* 16 (2010) 161–171.
- [53] A. Cociolo, F. Di Domenico, R. Coccia, A. Fiorini, J. Cai, W.M. Pierce, et al., Decreased expression and increased oxidation of plasma haptoglobin in Alzheimer disease: insights from redox proteomics, *Free Radic. Biol. Med.* 53 (2012) 1868–1876.
- [54] M.B. Pepys, T.W. Rademacher, S. Amatayakul-Chantler, P. Williams, G.E. Noble, W.L. Hutchinson, et al., Human serum amyloid P component is an invariant constituent of amyloid deposits and has a uniquely homogeneous glycostructure, *Proc. Natl. Acad. Sci. U. S. A.* 91 (1994) 5602–5606.
- [55] K. Yasojima, C. Schwab, E.G. McGeer, P.L. McGeer, Human neurons generate C-reactive protein and amyloid P: upregulation in Alzheimer's disease, *Brain Res.* 887 (2000) 80–89.
- [56] S. Janciauskiene, P. García de Frutos, E. Carlemalm, B. Dahlbäck, S. Eriksson, Inhibition of Alzheimer beta-peptide fibril formation by serum amyloid P component, *J. Biol. Chem.* 270 (1995) 26041–26044.
- [57] J.R. Crawford, N.L. Bjorklund, G. Tagliatalata, R.H. Gomer, Brain Serum Amyloid P Levels are Reduced in Individuals that Lack Dementia While Having Alzheimer's Disease, *Neuropathology Neurochem. Res.* 37 (2012) 795–801.
- [58] S.E. Kolstoe, B.H. Ridha, V. Bellotti, N. Wang, C.V. Robinson, S.J. Crutch, et al., Molecular dissection of Alzheimer's disease neuropathology by depletion of serum amyloid P component, *Proc. Natl. Acad. Sci. U. S. A.* 106 (2009) 7619–7623.
- [59] J.T. Rogers, A.I. Bush, H.H. Cho, D.H. Smith, A.M. Thomson, A.L. Friedlich, et al., Iron and the translation of the amyloid precursor protein (APP) and ferritin mRNAs: riboregulation against neural oxidative damage in Alzheimer's disease, *Biochem. Soc. Trans.* 36 (2008) 1282–1287.
- [60] A.A. Alkhateeb, J.R. Connor, The significance of ferritin in cancer: anti-oxidation, inflammation and tumorigenesis, *Biochim. Biophys. Acta* 2013 (1836) 245–254.
- [61] X. Zhang, N. Surguladze, B. Sagle-Webb, A. Cozzi, J.R. Connor, Cellular iron status influences the functional relationship between microglia and oligodendrocytes, *Glia* 54 (2006) 795–804.
- [62] M.M. Goyal, A. Basak, Human catalase: looking for complete identity, *Protein Cell* 1 (2010) 888–897.
- [63] N.G.N. Milton, Amyloid-beta binds catalase with high affinity and inhibits hydrogen peroxide breakdown, *Biochem. J.* 344 (1999) 293–296.

- [64] J. Luo, S.K. Wärmländer, A. Gräslund, J.P. Abrahams, Non-chaperone proteins can inhibit aggregation and cytotoxicity of Alzheimer amyloid β peptide, *J. Biol. Chem.* 289 (2014) 27766–27775.
- [65] L.K. Habib, M.T. Lee, J. Yang, Inhibitors of catalase-amyloid interactions protect cells from beta-amyloid-induced oxidative stress and toxicity, *J. Biol. Chem.* 285 (2010) 38933–38943.
- [66] R.A. Poynton, M.B. Hampton, Peroxiredoxins as biomarkers of oxidative stress, *Biochim. Biophys. Acta* 1840 (2014) 906–912.
- [67] T. Nystrom, J. Yang, M. Molin, Peroxiredoxins, gerontogenes linking aging to genome instability and cancer, *Genes Dev.* 26 (2012) 2001–2008.
- [68] I. Ibraqui, G. Kienda, J. Soeur, G. Faye, G. Baldacci, R.D. Kolodner, M.E. Huang, Peroxiredoxin Tsa1 is the key peroxidase suppressing genome instability and protecting against cell death in *Saccharomyces cerevisiae*, *PLoS Genet.* 5 (2009), e1000524.
- [69] H.M.V. Tang, K.L. Siu, C.M. Wong, D.Y. Jin, Loss of yeast peroxiredoxin Tsa1p induces genome instability through activation of the DNA damage checkpoint and elevation of dNTP levels, *PLoS Genet.* 5 (2009), e1000697.
- [70] M. Molin, J. Yang, S. Hanzén, M.B. Toledano, J. Labarre, T. Nystrom, Life span extension and H₂O₂ resistance elicited by caloric restriction require the peroxiredoxin Tsa1 in *Saccharomyces cerevisiae*, *Mol. Cell* 43 (2011) 823–833.
- [71] A.J. Weids, C.M. Grant, The yeast peroxiredoxin Tsa1 protects against protein-aggregate-induced oxidative stress, *J. Cell Sci.* 127 (2014) 1327–1335.
- [72] J.M. Flynn, S. Melov, SOD2 in mitochondrial dysfunction and neurodegeneration, *Free Radic. Biol. Med.* 62 (2013) 4–12.
- [73] M.E. De Leo, S. Borrello, M. Passantino, B. Palazzotti, A. Mordente, A. Daniele, et al., Oxidative stress and overexpression of manganese superoxide dismutase in patients with Alzheimer's disease, *Neurosci. Lett.* 250 (1998) 173–176.
- [74] C.A. Massaad, R.G. Pautler, E. Klann, Mitochondrial superoxide: a key player in Alzheimer's disease, *Aging (Albany NY)* 1 (2009) 758–761.
- [75] M. Anantharaman, J. Tangpong, J.N. Keller, M.P. Murphy, W.R. Markesbery, K.K. Kinningham, D.K. St Clair, Beta-amyloid mediated nitration of manganese superoxide dismutase: implication for oxidative stress in a APPNLH/NLH X PS-1P264L/P264L double knock-in mouse model of Alzheimer's disease, *Am. J. Pathol.* 168 (2006) 1608–1618.
- [76] J.D. Hayes, D.J. Pulford, The glutathione S-transferase supergene family: regulation of GST and the contribution of the isoenzymes to cancer chemoprotection and drug resistance, *Crit. Rev. Biochem. Mol. Biol.* 30 (1995) 445–600.
- [77] H. Raza, Dual localization of glutathione S-transferase in the cytosol and mitochondria: implications in oxidative stress, toxicity and disease, *FEBS J.* 278 (2011) 4243–4251.
- [78] K.D. Tew, D.M. Townsend, Glutathione-S-transferases as determinants of cell survival and death, *Antioxid. Redox Signal.* 17 (2012) 1728–1737.
- [79] K.H. Sun, K.H. Chang, S. Clawson, S. Ghosh, H. Mirzaei, F. Regnier, K. Shah, Glutathione-S-transferase P1 is a critical regulator of Cdk5 kinase activity, *J. Neurochem.* 118 (2011) 902–914.
- [80] M. Qi, E.A. Elion, MAP kinase pathways, *J. Cell Sci.* 118 (2005) 3569–3572.
- [81] A. Chevrollier, D. Loiseau, P. Reynier, G. Stepien, Adenine nucleotide translocase 2 is a key mitochondrial protein in cancer metabolism, *Biochim. Biophys. Acta* 2011 (2011) 562–567.
- [82] M. Morán, D. Moreno-Lastres, L. Marín-Buena, J. Arenas, M.A. Martín, C. Ugalde, Mitochondrial respiratory chain dysfunction: implications in neurodegeneration, *Free Radic. Biol. Med.* 53 (2012) 595–609.
- [83] G.E. Gibson, A. Starkov, J.P. Blass, R.R. Ratan, M.F. Beal, Cause and consequence: mitochondrial dysfunction initiates and propagates neuronal dysfunction, neuronal death and behavioral abnormalities in age-associated neurodegenerative diseases, *Biochim. Biophys. Acta* 1802 (2010) 122–134.
- [84] M. Frenzel, H. Rommelspacher, M.D. Sugawa, N.A. Dencher, Ageing alters the supramolecular architecture of OxPhos complexes in rat brain cortex, *Exp. Gerontol.* 45 (2010) 563–572.
- [85] A.M. Stranahan, M.P. Mattson, Recruiting adaptive cellular stress responses for successful brain ageing, *Nat. Rev. Neurosci.* 13 (2012) 209–216.
- [86] Y. Mizuno, S. Ohta, M. Tanaka, S. Takamiya, K. Suzuki, T. Sato, et al., Deficiencies in complex I subunits of the respiratory chain in Parkinson's disease, *Biochem. Biophys. Res. Commun.* 163 (1989) 1450–1455.
- [87] S.H. Kim, R. Vlkolinsky, N. Cairns, M. Fountoulakis, G. Lubec, The reduction of NADH ubiquinone oxidoreductase 24- and 75-kDa subunits in brains of patients with Down syndrome and Alzheimer's disease, *Life Sci.* 68 (2001) 2741–2750.
- [88] D. Li, H. Chen, A. Florentino, D. Alex, P. Sikorski, W.A. Fonzi, R. Calderone, Enzymatic dysfunction of mitochondrial complex I of the *Candida albicans* goa1 mutant is associated with increased reactive oxidants and cell death, *Eukaryot. Cell* 10 (2011) 672–682.
- [89] F. Bosetti, F. Brizzi, S. Barogi, M. Mancuso, G. Siciliano, E.A. Tendi, et al., Cytochrome c oxidase and mitochondrial F1F0-ATPase (ATP synthase) activities in platelets and brain from patients with Alzheimer's disease, *Neurobiol. Aging* 23 (2002) 371–376.
- [90] V. Marshansky, J.L. Rubinstein, G. Grüber, Eukaryotic V-ATPase: novel structural findings and functional insights, *Biochim. Biophys. Acta* 1837 (2014) 857–879.
- [91] Y. Fujita, T. Yamashita, Axon growth inhibition by RhoA/ROCK in the central nervous system, *Front. Neurosci.* 8 (2014) 338, <http://dx.doi.org/10.3389/fnins.2014.00338>.
- [92] B. Pianu, R. Lefort, L. Thuilliere, E. Tabourier, F. Bartolini, The A β _{1–42} peptide regulates microtubule stability independently of tau, *J. Cell Sci.* 127 (2014) 1117–1127.
- [93] Y. Yoshikumi, H. Mashima, N. Ueda, H. Ohno, J. Suzuki, S. Tanaka, et al., Roles of CTPL/Sfxn3 and Sfxn family members in pancreatic islet, *J. Cell. Biochem.* 95 (2005) 1157–1168.
- [94] X. Li, D. Han, R. Kin Ting Kam, X. Guo, M. Chen, Y. Yang, H. Zhao, Y. Chen, Developmental expression of sideroflexin family genes in *Xenopus* embryos, *Dev. Dyn.* 239 (2010) 2742–2747.
- [95] P. Mookherjee, P.S. Green, G.S. Watson, M.A. Marques, K. Tanaka, K.D. Meeker, et al., GLT-1 loss accelerates cognitive deficit onset in an Alzheimer's disease animal model, *J. Alzheimers Dis.* 26 (2011) 447–455.
- [96] T. Cassano, G. Serviddio, S. Gaetani, A. Romano, P. Dipasquale, S. Cianci, et al., Glutamatergic alterations and mitochondrial impairment in a murine model of Alzheimer disease, *Neurobiol. Aging* 33 (2012) 1121.e1–1121.e12.
- [97] M.M. Dorostkar, S. Burgold, S. Filser, S. Barghorn, B. Schmidt, U.R. Anumala, et al., Immunotherapy alleviates amyloid-associated synaptic pathology in an Alzheimer's disease mouse model, *Brain* 137 (2014) 3319–3326.
- [98] D. Yuki, Y. Sugiura, N. Zaima, H. Akatsu, S. Takei, I. Yao, et al., DHA-PC and PSD-95 decrease after loss of synaptophysin and before neuronal loss in patients with Alzheimer's disease, *Sci Rep* 4 (2014) 7130.
- [99] M. Shinohara, S. Fujioka, M.E. Murray, A. Wojtas, M. Baker, A. Rovelet-Lecrux, et al., Regional distribution of synaptic markers and APP correlate with distinct clinicopathological features in sporadic and familial Alzheimer's disease, *Brain* 137 (2014) 1533–1549.
- [100] A. Savioz, G. Leuba, P.G. Vallet, A framework to understand the variations of PSD-95 expression in brain aging and in Alzheimer's disease, *Ageing Res. Rev.* 18 (2014) 86–94.
- [101] K.D. Meeker, J.S. Meabon, D.G. Cook, Partial loss of the glutamate transporter GLT-1 alters brain Akt and insulin signaling in a mouse model of Alzheimer's disease, *J. Alzheimers Dis.* 45 (2015) 509–520.
- [102] M.V. Zelaya, E. Pérez-Valderrama, X.M. de Morentin, T. Tuñon, I. Ferrer, M.R. Luquin, et al., Olfactory bulb proteome dynamics during the progression of sporadic Alzheimer's disease: identification of common and distinct olfactory targets across Alzheimer-related co-pathologies, *Oncotarget* 6 (2015) 39437–39456, <http://dx.doi.org/10.18632/oncotarget.6254>.
- [103] J. Ho Kim, J. Franck, T. Kang, H. Heinsen, R. Ravid, I. Ferrer, et al., Proteome-wide characterization of signalling interactions in the hippocampal CA4/DG subfield of patients with Alzheimer's disease, *Sci. Rep.* 5 (2015) 11138, <http://dx.doi.org/10.1038/srep11138>.